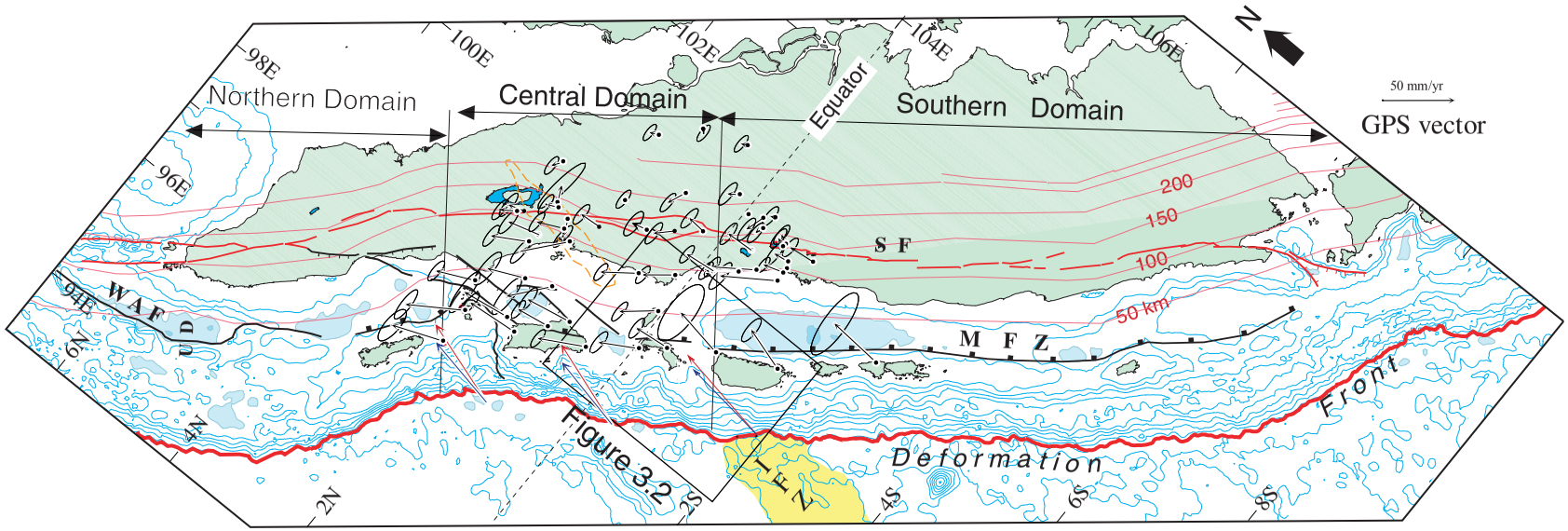

Figure 3.1 Map of the principal tectonic elements of the Sumatran plate boundary. Oblique subduction of the Indian-Australian plate beneath Sumatra is accommodated by frontal slip on the subduction interface and by the dextral Sumatran fault. It can be divided into three tectonic domains. In the southern domain, the trench-slope break, outer-arc ridge, fore-arc basin and Sumatran fault are the least irregular. In the Central domain, the fore-arc region is splintered by secondary faults, and the Sumatran fault strikes markedly across the subduction isobaths. The Investigator fracture zone (IFZ) is subducting beneath the Central domain. These structural features seem to play a role in determining the source parameters of large earthquakes and the degree of coupling of the subduction interface. Black arrows are GPS-derived velocity vectors with 95% confidence ellipses relative to eastern Sumatra (SE Asia), from 1989-94 GPS campaigns [Prawirodirdjo et al, 1997; McCaffrey, 2000]. Arrows at trench are plate convergence vectors, the more northerly of each pair (red arrows) are from the Australia - Eurasia pole of Larson et al. [1997] and the blue ones are from the NUVEL-1A Australia - Eurasia pole of DeMets et al. [1994]. Results from the 2001 campaign [Bock et al, 2001] are not shown, but appear to show less of a trench-parallel component north of the Equator. Orange-dashed ellipse is a N-S trending high seismicity zone. MFZ=Mentawai fault zone. WAF=West Andaman fault zone. SF=Sumatran Fault.

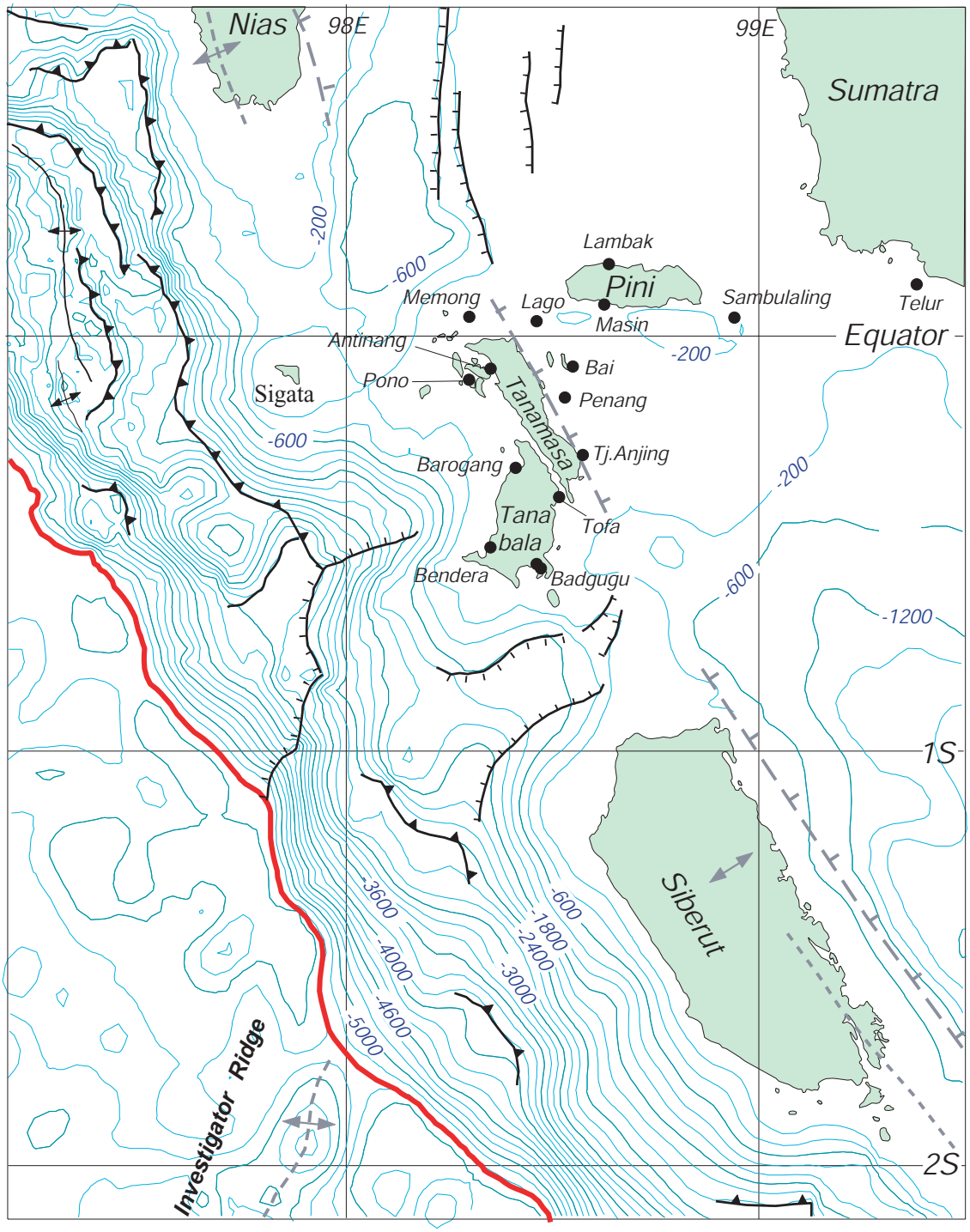

Figure 3.2 Index map to the coral paleogeodetic sites. Bathymetry and tectonic framework of the central Sumatran subduction is adapted from Chapter 2.

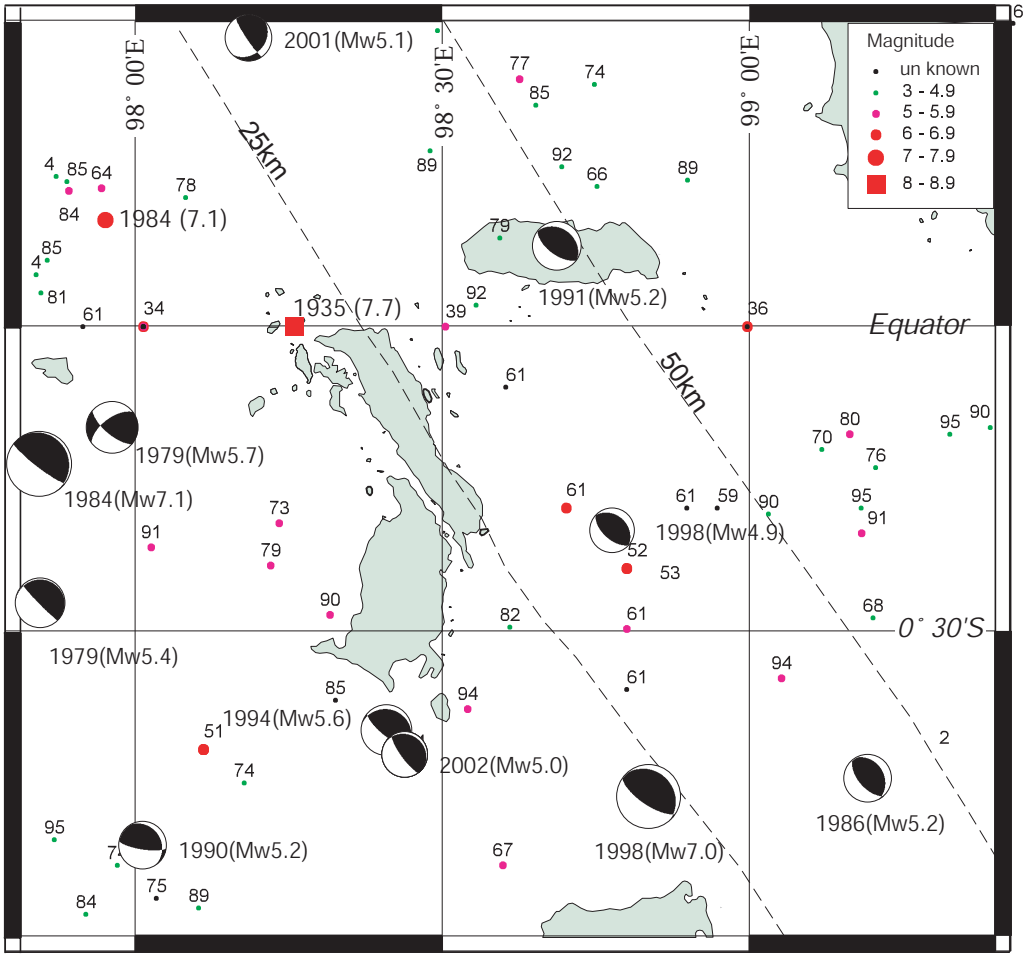

Figure 3.3 Seismicity in the central Sumatran subduction zone. Dots are earthquake epicenter with color coded magnitudes. Numbers next to dots are years. Epicenter data from 1900 to 1963 are from NEIC catalogue. Epicenters from 1964 to 1998 are from Engdahl's [1998] relocations. The beach balls are Harvard double-couple solutions for earthquakes between January 1976 and October 2002.

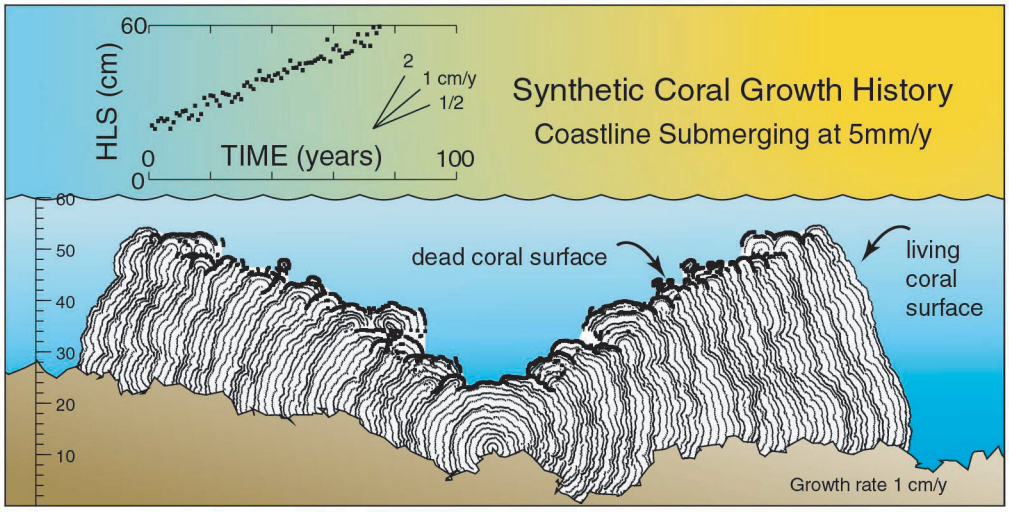

Figure 3.4a The computer simulation of 100 years of growth of a coral microatoll located in a submerging area. Submergence is steady at 5 mm/yr. Input coral growth rate is 10 mm/yr. HLS values in the graphic are the sum of long-term submergence and random Gaussian variables with zero mean and ± 2 cm standard deviation, but are not necessarily recorded by the HLS impingement upon the coral growth. The bold black lines indicate where the tops of coral growth are impinged by HLS. The main feature is that the microatoll develops a cup-shaped morphology.

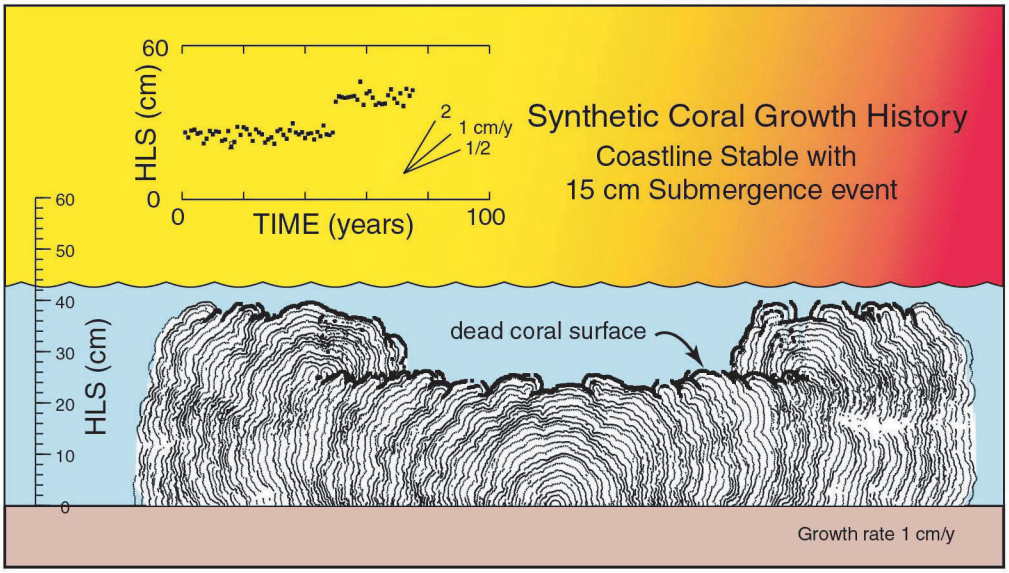

Figure 3.4b The computer generated simulation for a microatoll located in a stable region, but which experiences a sudden submergence of about 15 cm in the 50th year. Coral micro-topography evolves lower and upper flat surfaces separated by a step of rapid and unrestricted coral growth between the 50th and the 60th years. Note that coral stratigraphy is devoid of HLS record between the inception of submergence at year 50 and the first impingement of coral growth at about year 1962. However it does record the minimum value of HLS (HLS minima).

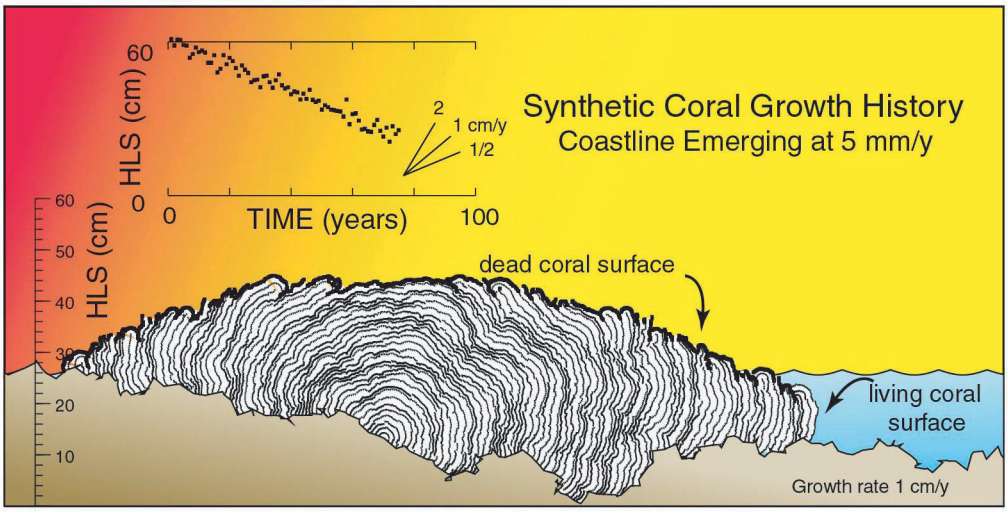

Figure 3.4c This synthetic microatoll is located on an intertidal reef that is emerging at 5 mm/yr. The coral's upper surface shows a descending growth pattern. Cusps and swales ornamenting the surface represent random annual sea-level fluctuations. The typical coral morphology in this environment is a dome shape.

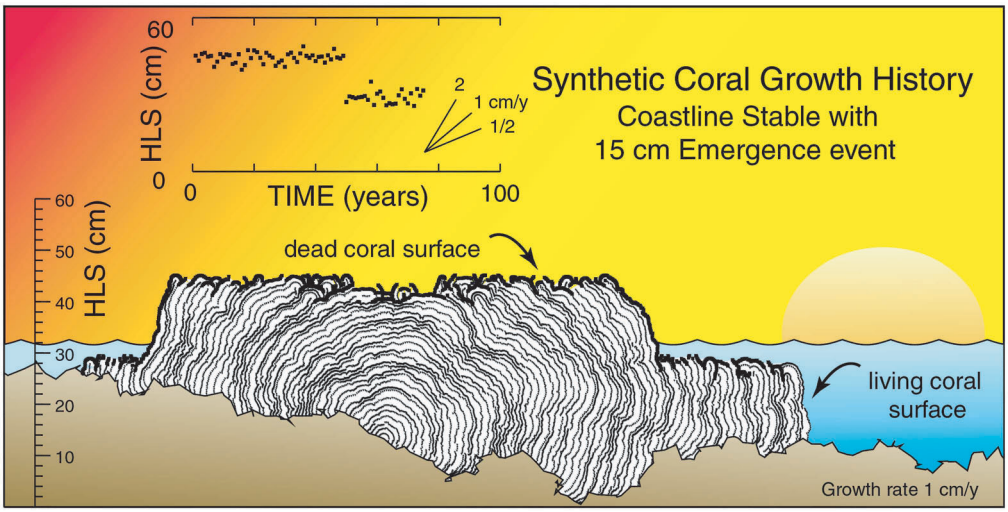

Figure 3.4d. In this computer simulation, the site has a long-term stability but the coral experiences a sudden 15-cm emergence event in year 50. This "short-duration" vertical deformation causes a permanent change in sea level; thus the microatoll develops a hat-shaped morphology.

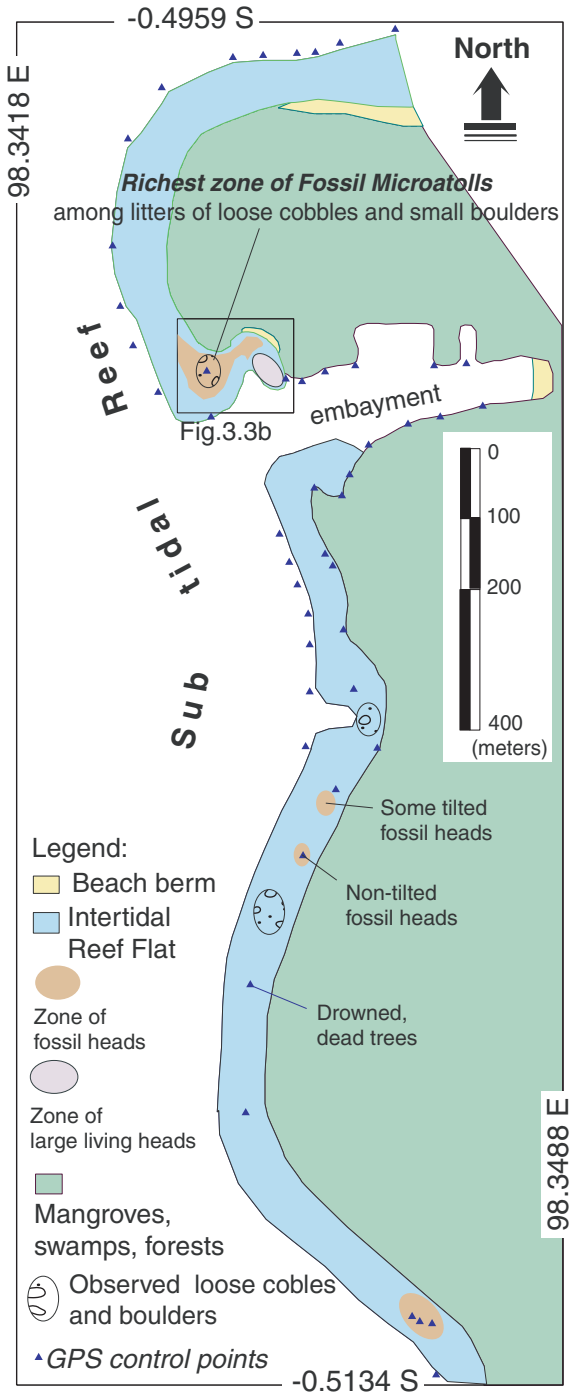

Figure 3.5a General site map at Bendera bay, southwest Tanabala.

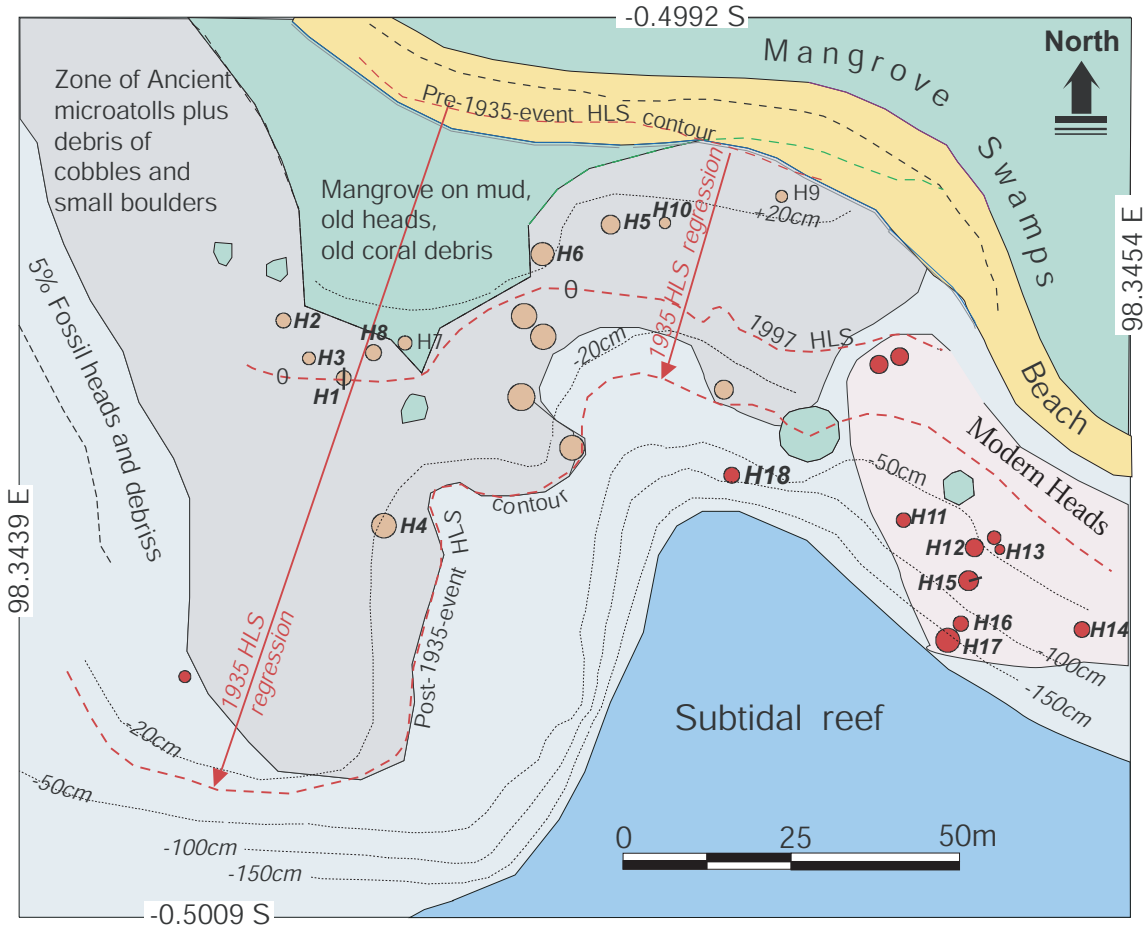

Figure 3.5b. Detailed site map. Sudden emergence during the 1935 event raised the enterity of the intertidal reef above the lowest tide level and killed the ancient microatolls (indicated by red arrows). Solid bars on H1 and H15 are coral slabs collected in mid-1997 and mid-2000 field survey.

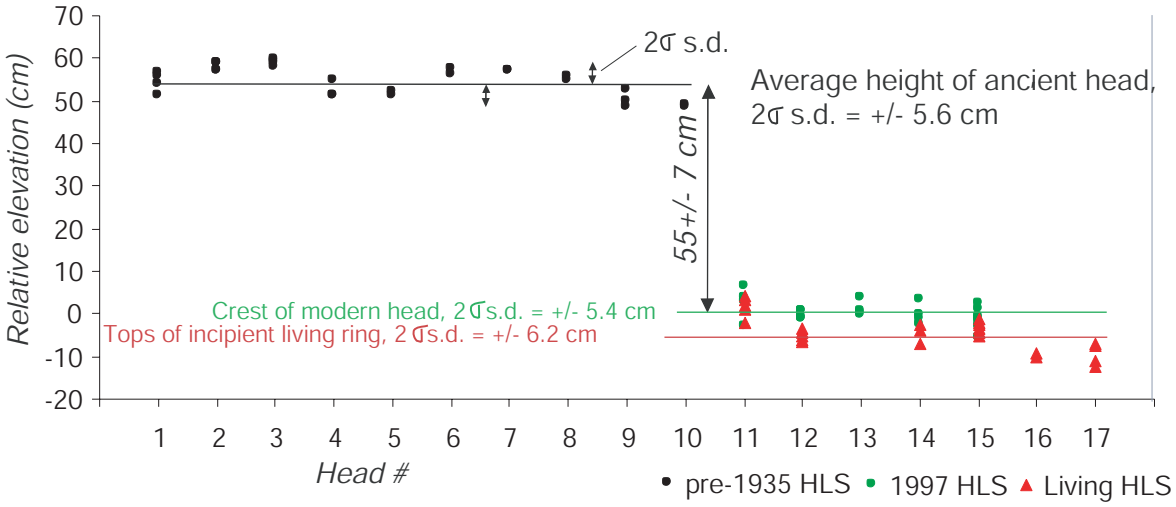

Figure 3.6a Elevations of perimeter crests of the ancient and the living microatolls. The difference in their heights implies that at least about 55 cm of emergence occurred in the 1935 event.

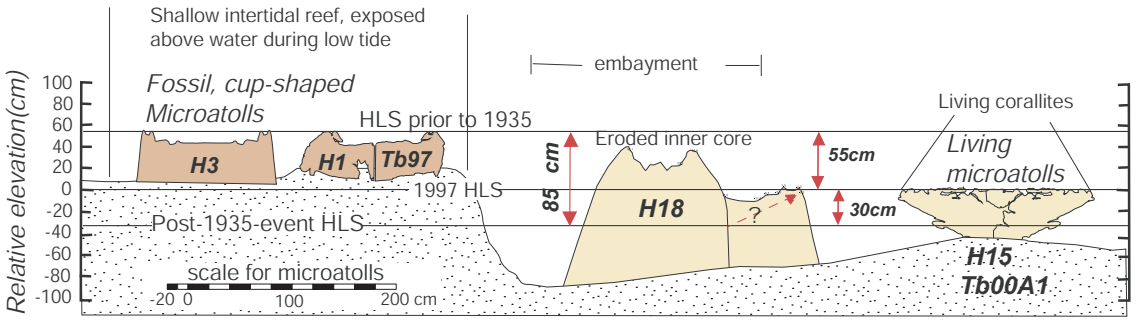

Figure 3.6b Shapes and relative positions of the three types of microatolls in Bendera site. Fossil microatolls rose entirely above the intertidal zone during the 1935 event and died. H18 was only partially exposed, so that the lower part survived the event.

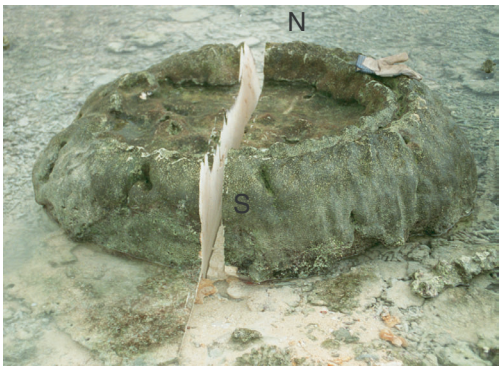

Figure 3.7a Sampled ancient microatoll (H1). The cup-shaped geometry implies that a rapid submergence had occurred prior to the 1935 event.

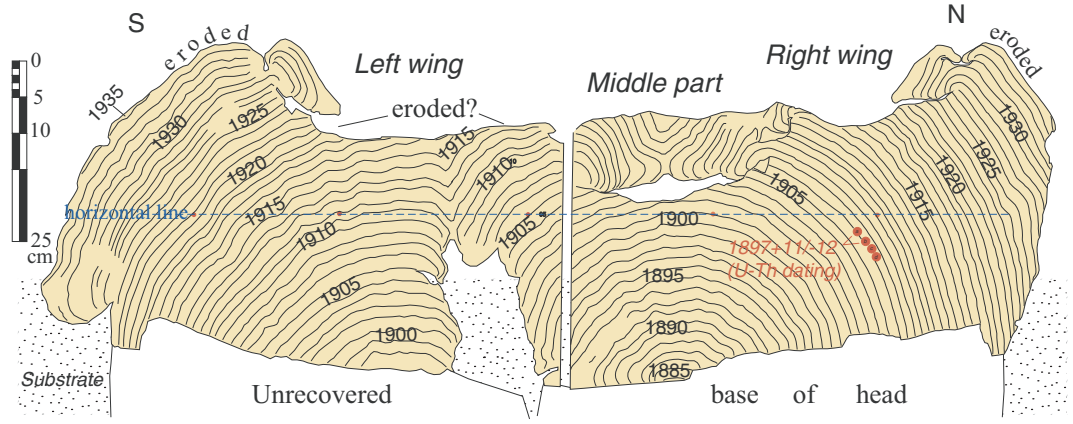

Figure 3.7b Drawing of the Tb97 slab collected from H1. The diameter cross section permits the comparison of HLS histories from the two radiuses. The annual banding is exceptionally clear, so there are no ambiguities in the relative ages. The age assignment assumes the final death in 1935.

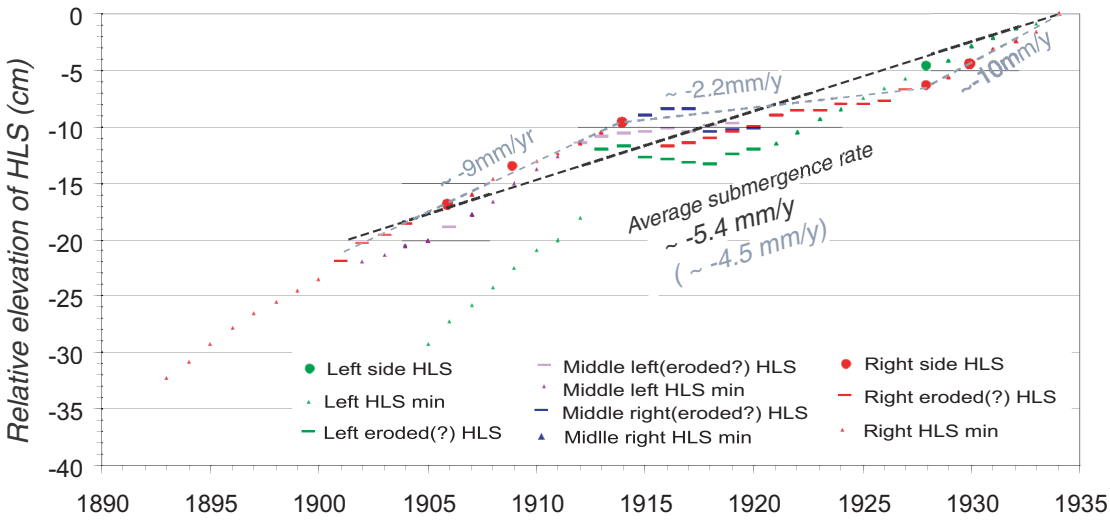

Figure 3.7c HLS records recovered from the Tb97 are plotted as a function of time. The averaged submergence rates are determined by the least squares fits of the entire or partial HLS records. The least-squares fit to all the HLS record from 1900 to 1935 yields 5.4 mm/yr submergence; if using only preserved HLS it yields 4.5 mm/yr submergence.

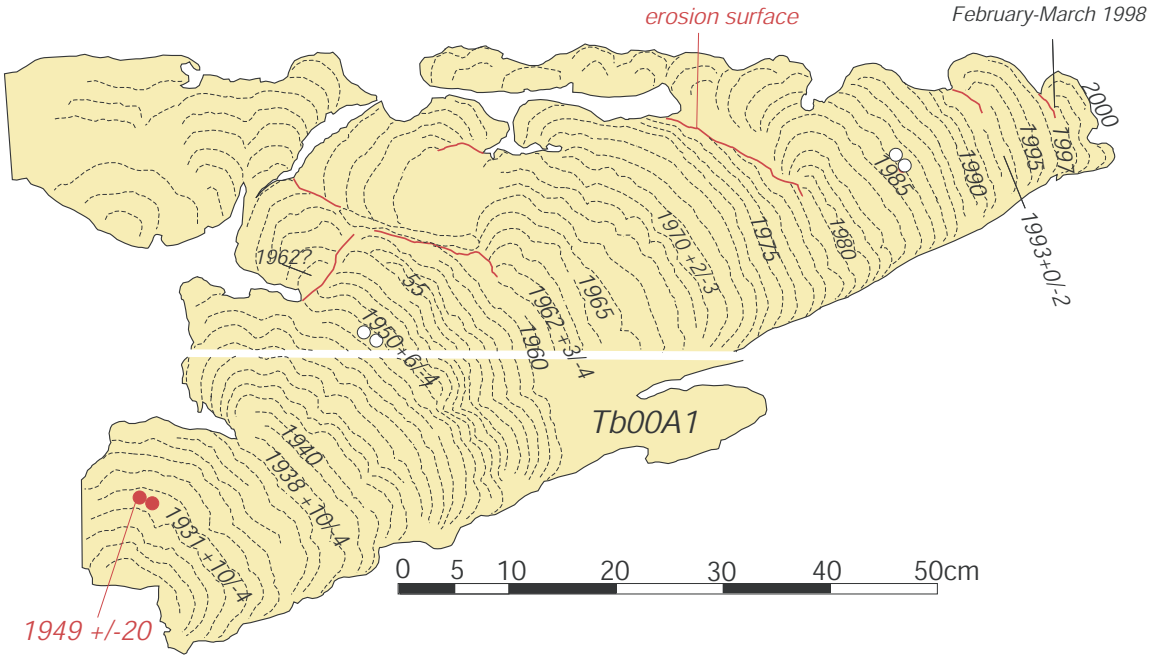

Figure 3.8a Drawing of the radiograph of the Tb00A1 thin section. Overall stratigraphy indicates fast submergence since about the mid-1930s. HLS impingements occurred in 1955, 1962, mid-1970s, early 1980s, early to mid-1990s, and in 1997 or early 1998.

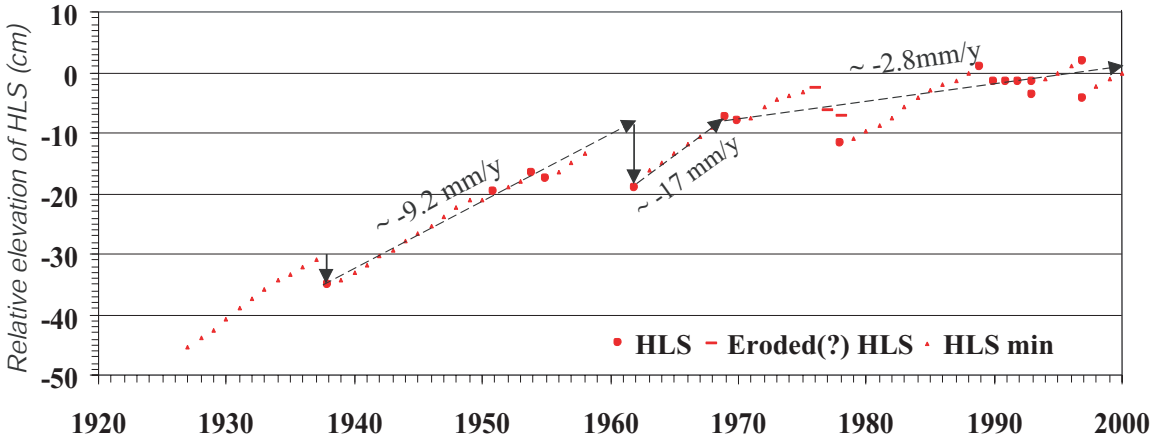

Figure 3.8b HLS records recovered from the Tb97 are plotted as a function of time. The averaged submergence rates are determined by the least-squares fits of the entire or partial HLS records. The least-squares fit to all the HLS record from 1900 to 1935 yields 5.4 mm/yr submergence; if using only preserved HLS it yields 4.5 mm/yr submergence.

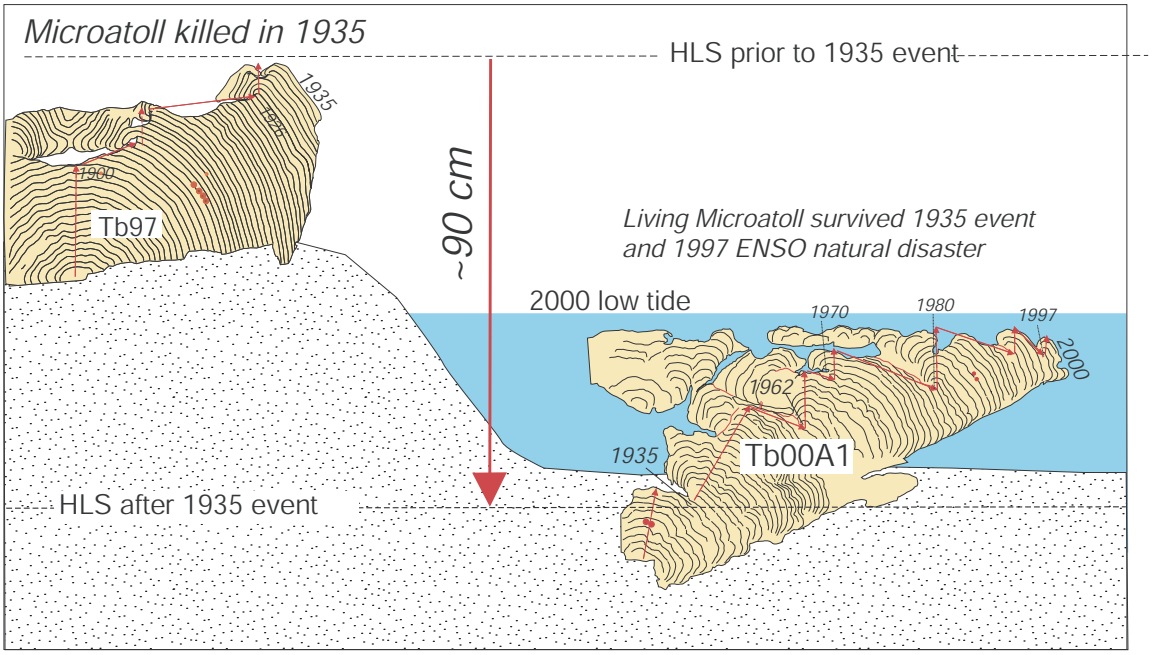

Figure 3.9a Schematic diagram showing a combine coral stratigraphy from Tb97 and from Tb00A1 slabs. The principal feature is the record of the full emergence in 1935 that is measured from the crest of the ancient head's exterior to the first HLS clip in the modern microatoll.

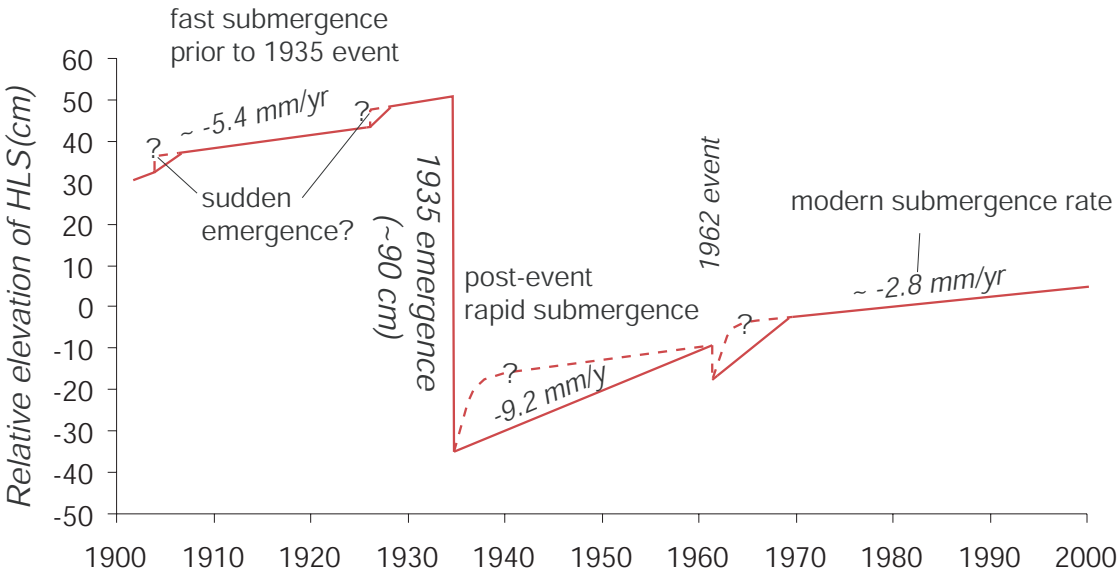

Figure 3.9b The combine HLS history recovered from The ancient and the living heads span the entire 20th century. The 1935 emergence event dominates the history. A period of submergence prior to 1935 appears to be eventful. The fastest submergence rate occurred in a period after the 1935 event. The 1962 event is the second largest feature, and marked a decline in the submergence rate.

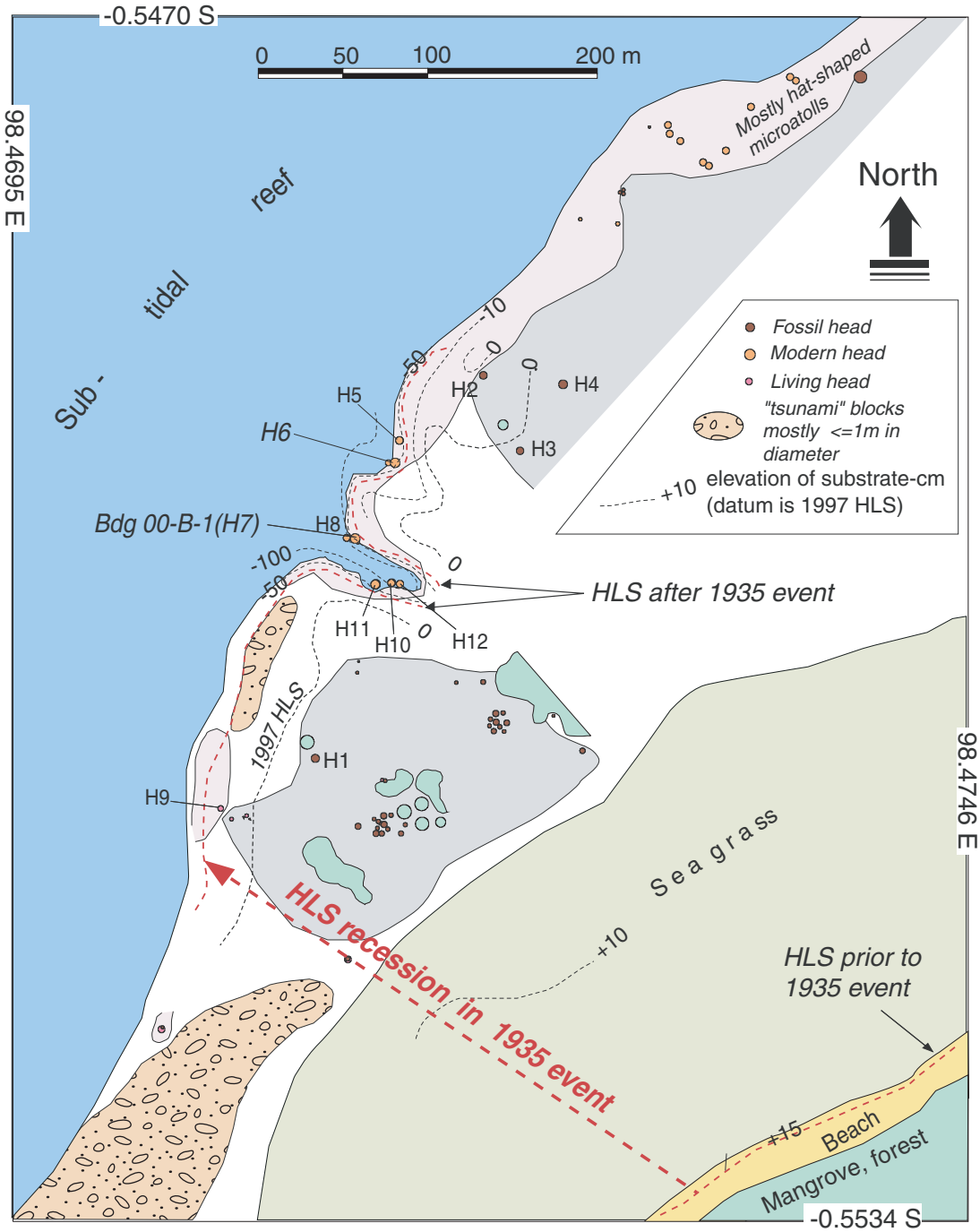

Figure 3.10 Map of east Badgugu site.

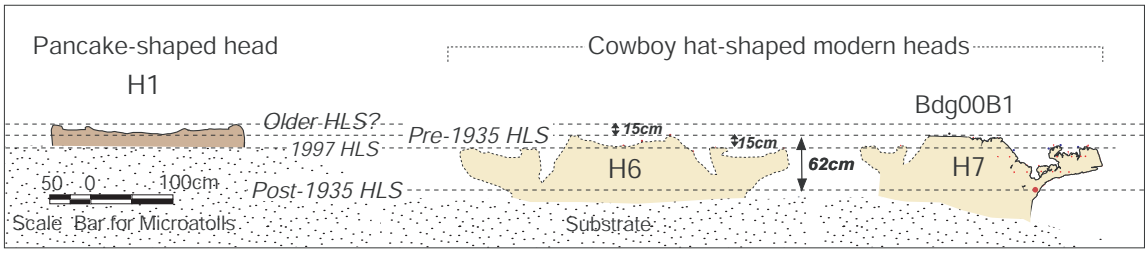

Figure 3.11a Schematic beach cross-section and the two populations of microatolls.

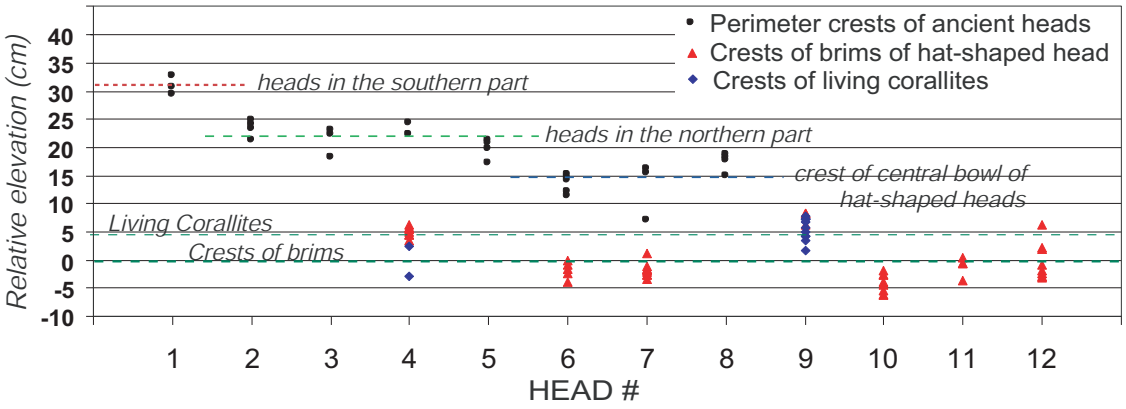

Figure 3.11b Relative elevations of tops of microatoll's perimeters.

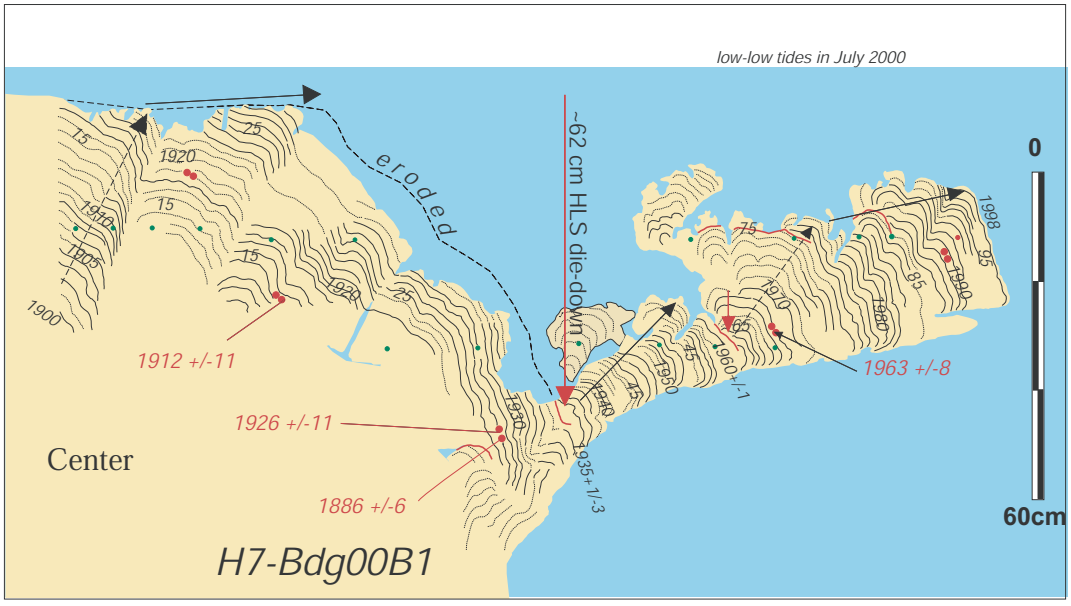

Figure 3.12a Cross section of the Bdg00B1 slab. The HLS die-down between the central bowl and the brim represents the emergence during the 1935 event. The central bowl consists of coral bands that had grown prior to 1935. The brim consists of growth bands after 1935.

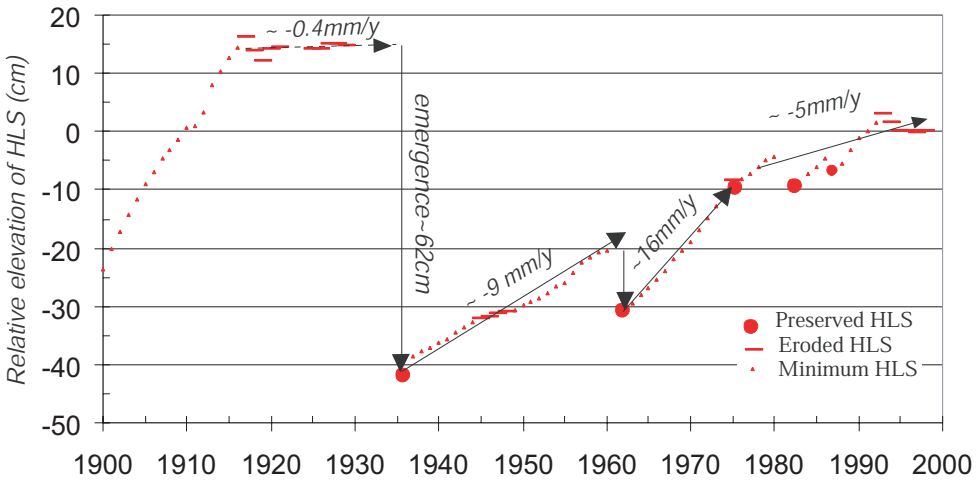

Figure 3.12b HLS history of Bdg00B1 slab from east Badgugu site.

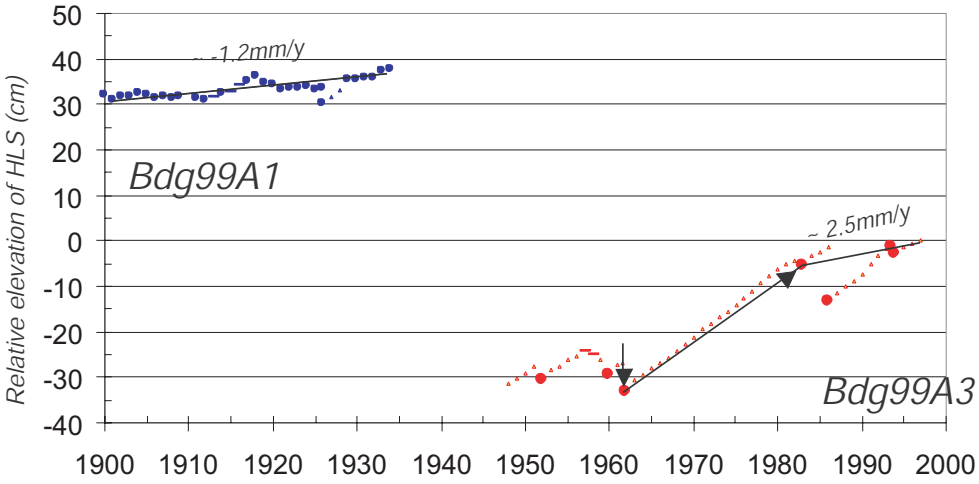

Figure 3.13 HLS history from west Badgugu site.

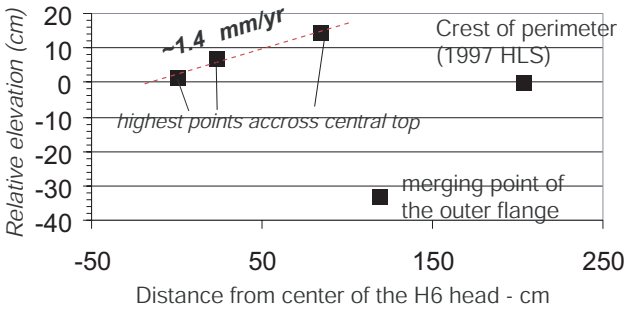

Figure 3.14 Surveyed crest points of the head H6 from the center to exterior.

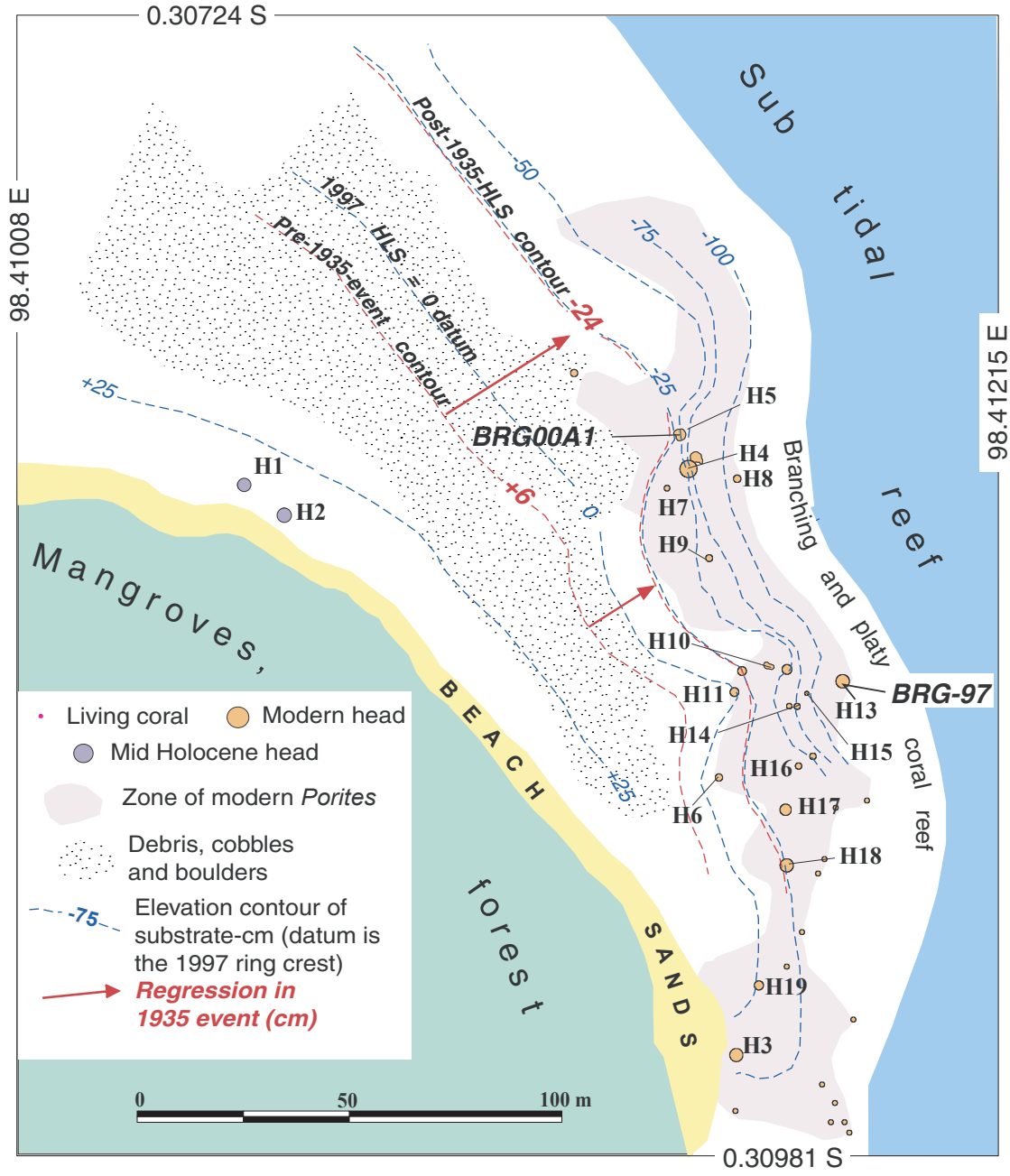

Figure 3.15 Barogang site map. During the 1935 event the intertidal reef rose about 30 cm, thus lowering HLS from +6 cm above to -24 cm below the 1997 ring crest. Numerous modern heads display the hat-shaped morphology that testifies to the 1935 emergence.

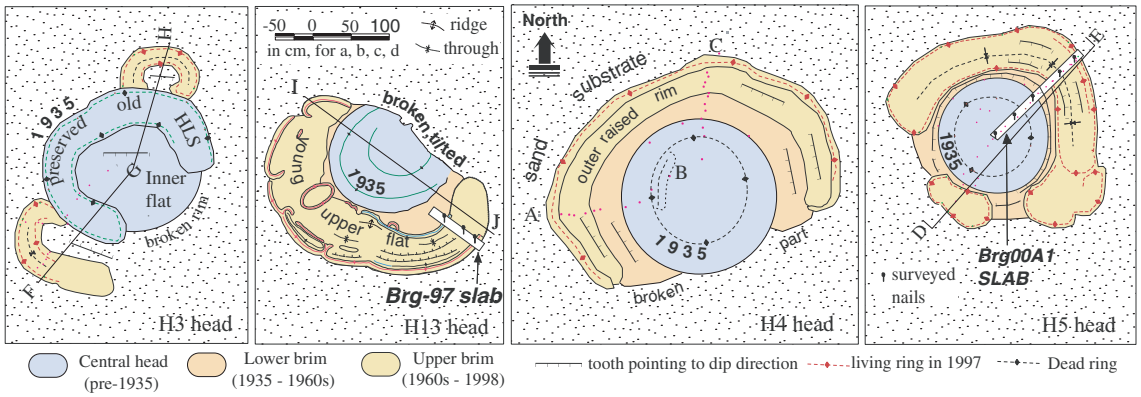

Figure3.16a Detailed map of the modern hat-shaped microatolls.

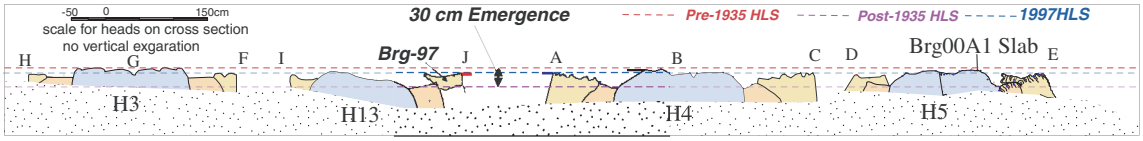

Figure 3.16b Cross sections of the modern hat-shaped microatolls. The head consist of three principal parts: central bowl, lower brim, and upper brim.

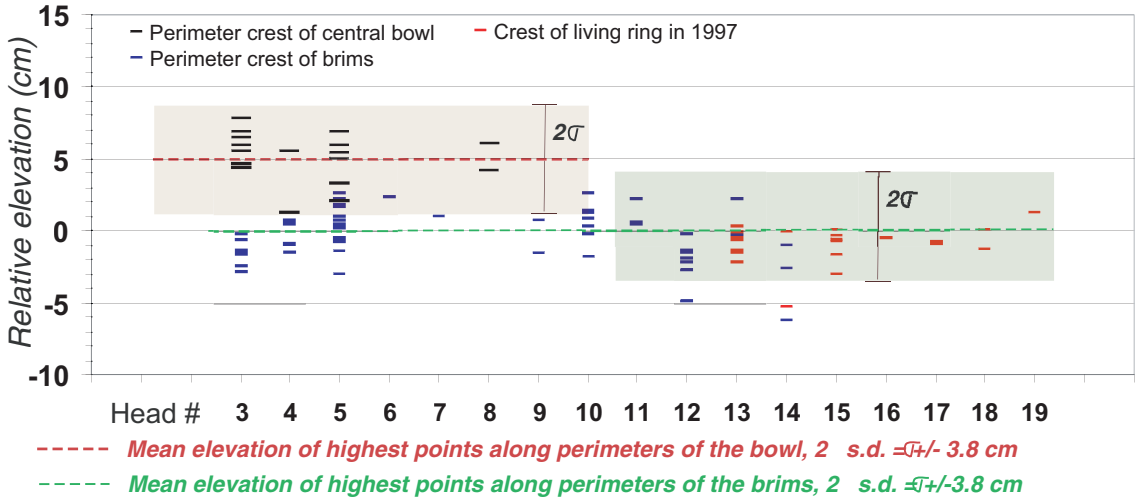

Figure 3.16c Elevations of the perimeter crests of the central bowl and the brims. The red bars are crests of the living exterior of the brim surveyed in mid-1997 when the heads were still alive. Difference in heights of the bowl and the brim indicates the emergence event during the course of the growth.

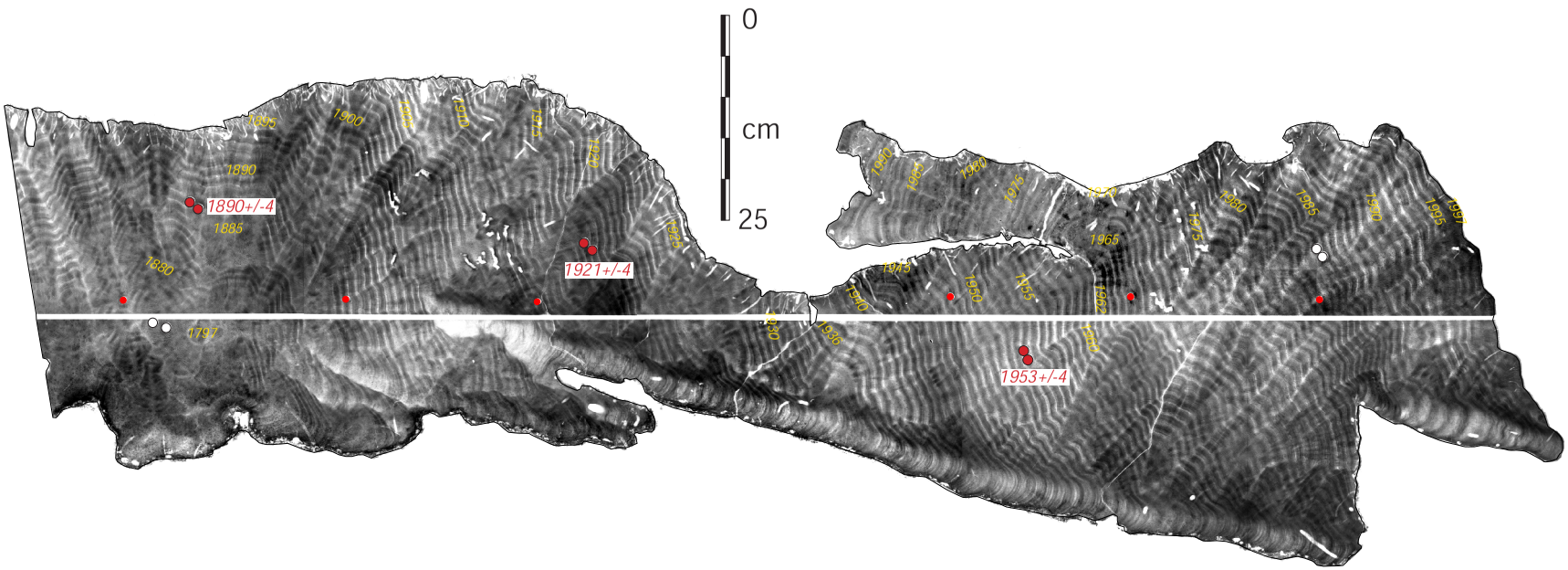

Figure 3.17a X-radiograph of the Brg00A1 slab showing excellent contrast of annual pairs of dark and light bands. This allows no ambiguity in visual ring counting.

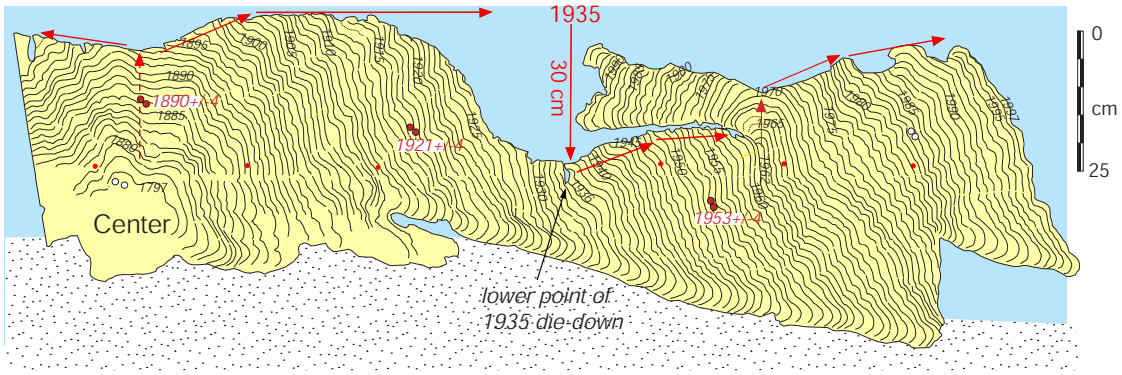

Figure 3.17b Drawing of the BrG00A1 X-radiograph showing the coral band stratigraphy of the hat-shaped head. An emergence of about 30 cm during the 1935 event killed the upper-half of the central bowl. The brim's topography indicates general fast submergence from 1935 until recently. Significant erosions occurred around the bowl removing much of the upper parts of bands 1920 to 1935.

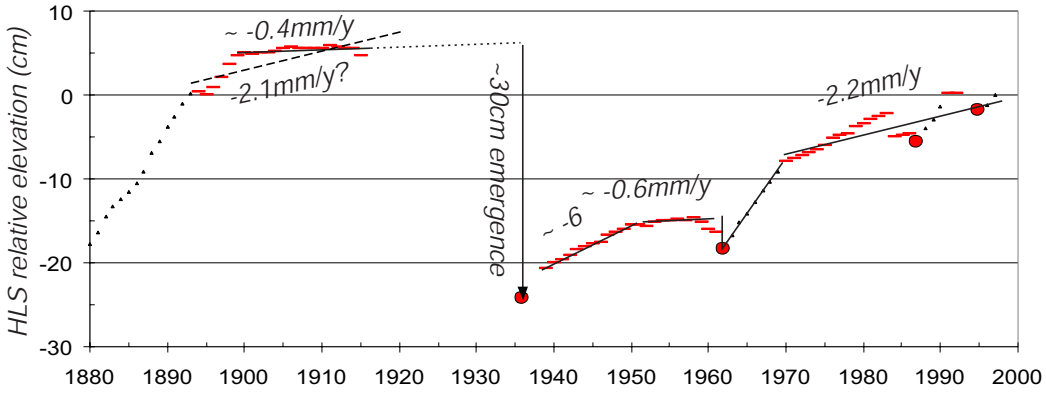

Figure 3.17c HLS history reconstructed from the Brg00A1 slab. A relatively stable period persisted for a few decades prior to 1935. Rapid submergence followed the 1935 event. Submergence appears to have decayed gradually to a much lower rate prior to 1961. The rapid or sudden submergence in 1962 is the second largest event in the history.

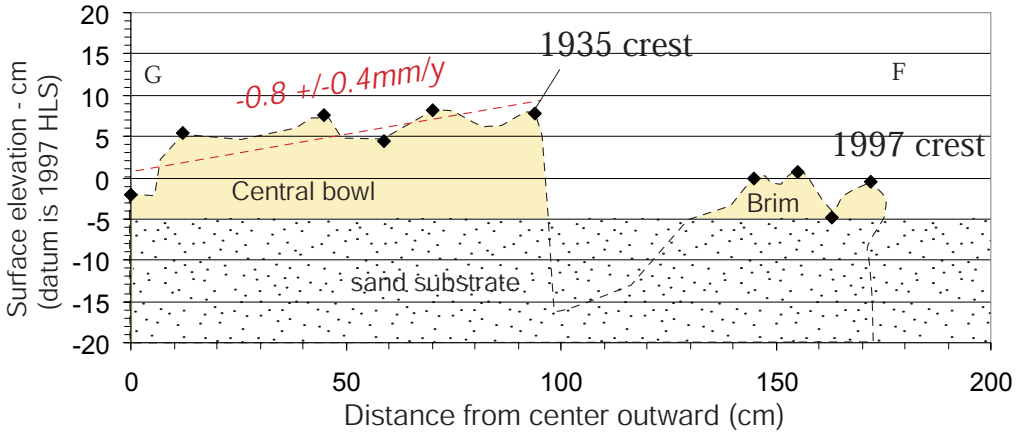

Figure 3.18 Topography of H3 that has a relatively preserved upper surface of the central bowl. A least squares fit to the surveyed points represents the best estimate for the rate prior to 1935.

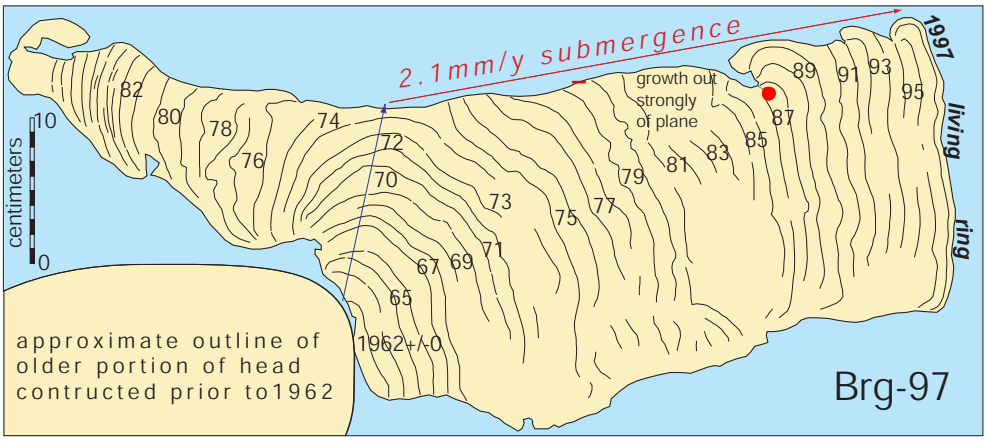

Figure 3.19a Coral stratigraphy of The Brg97 slab showing submergence event in 1962. HLS impingement from1974 to 1997 yields submergence rate of about 2.1mm/y.

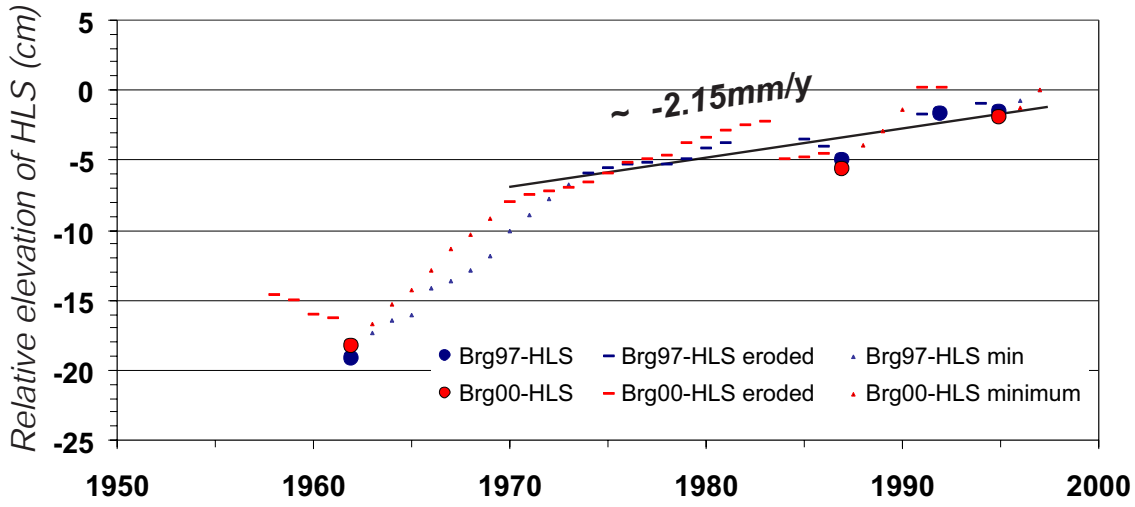

Figure 3.19b Combined HLS histories of Brg97 and Brg00A1 for the period from 1955 to 1997. It shows that the two HLS records from two different heads at this site are identical.

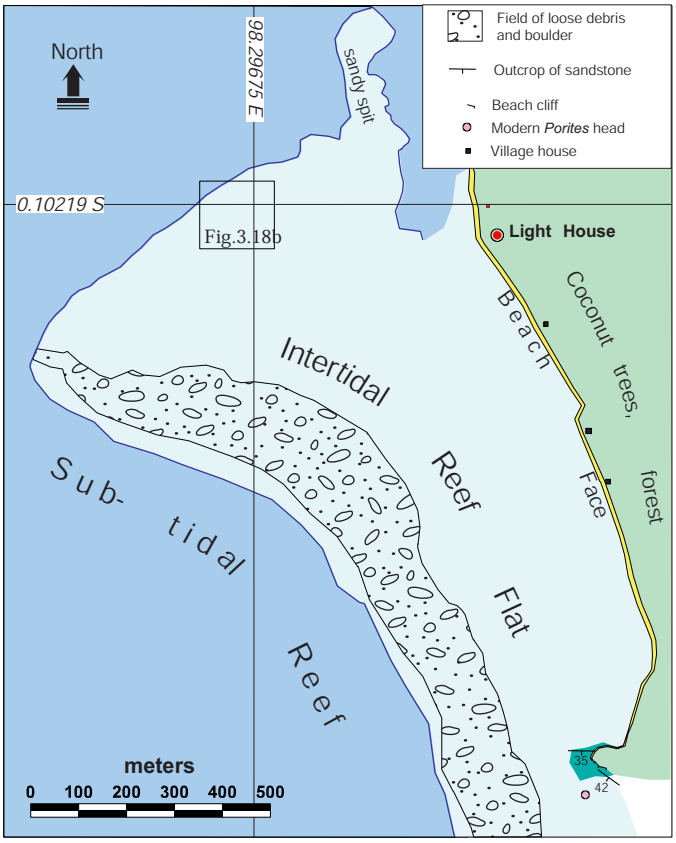

Figure 3.20a General map of Pono site.

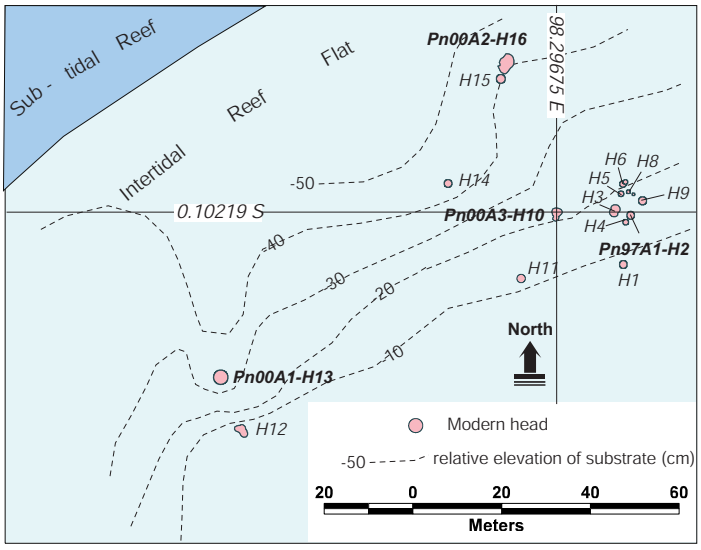

Figure 3.20b Detailed map of the surveyed microatolls.

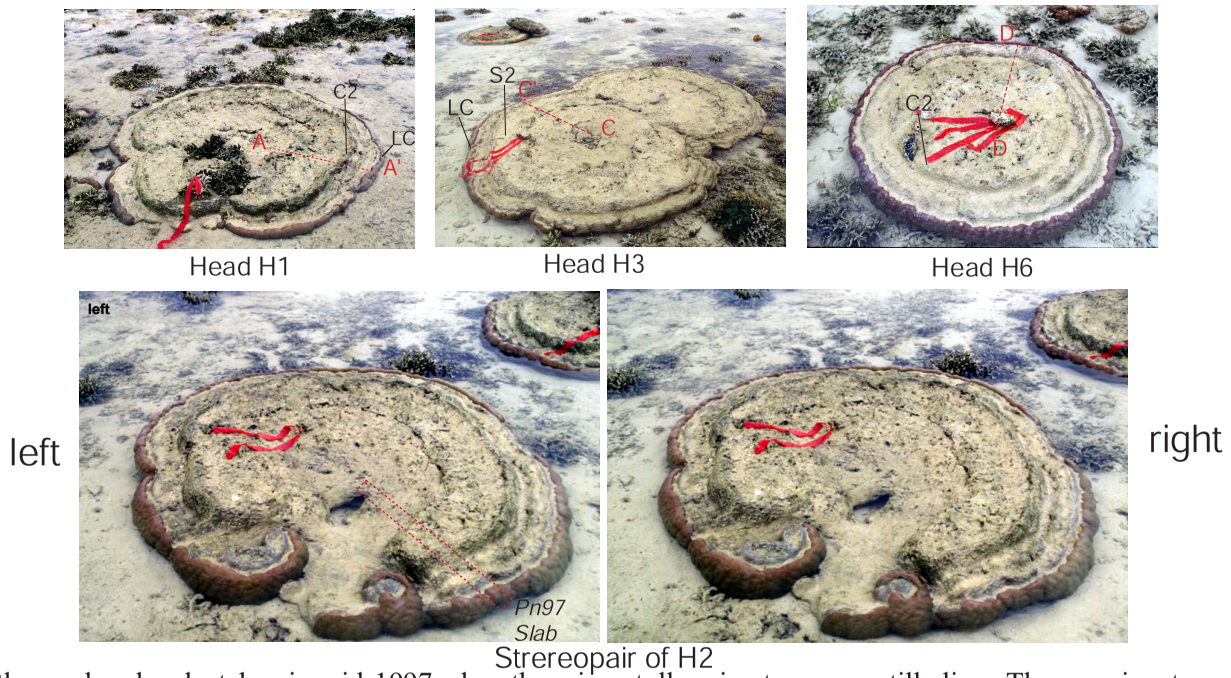

Figure 3.21a Photos of the modern heads, taken in mid-1997 when the microatoll perimeters were still alive. The prominent concentric terraces represent minor fluctuations in HLS and indicate heads have experienced only minor surface erosion. Outward down-stepping of the terraces implies emergence. See text for more discussion.

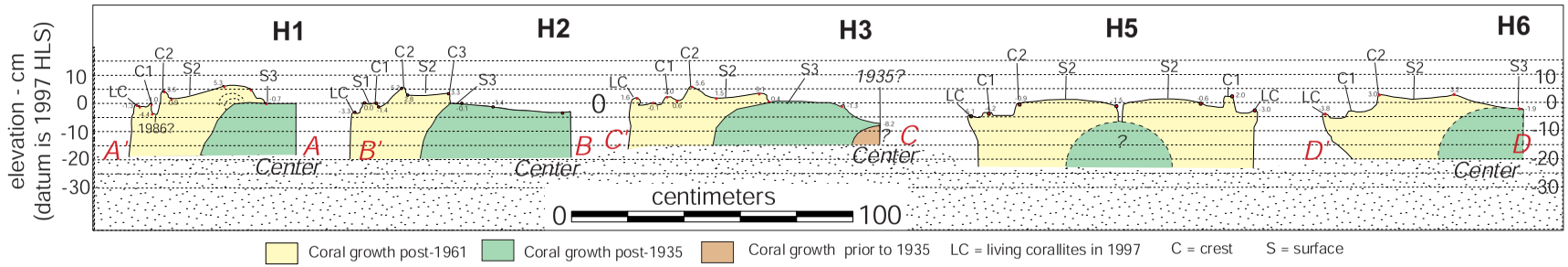

Figure 3.21b Cross sections of the selected modern heads above (except H5) showing lower central flats and prominent emergence for the past few decades.

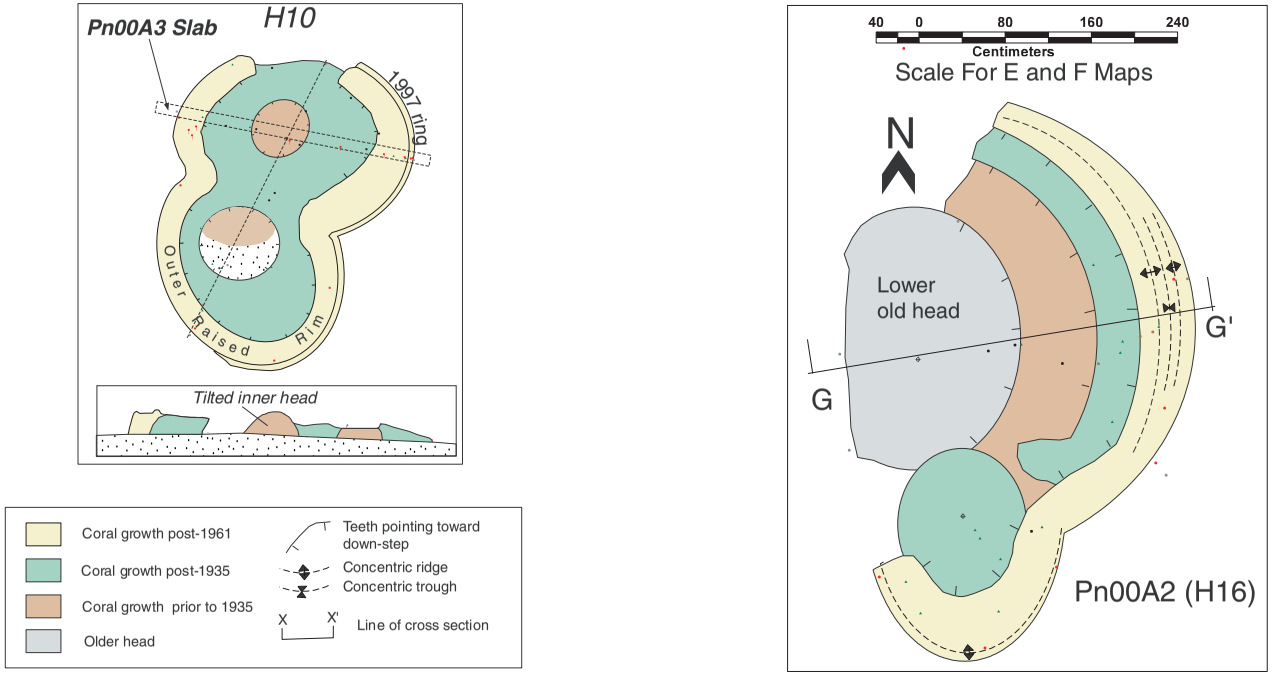

Figure 3.22a Plan-view maps of the large microatolls. Their topography shows a very low relief indicative of a general near stable condition.

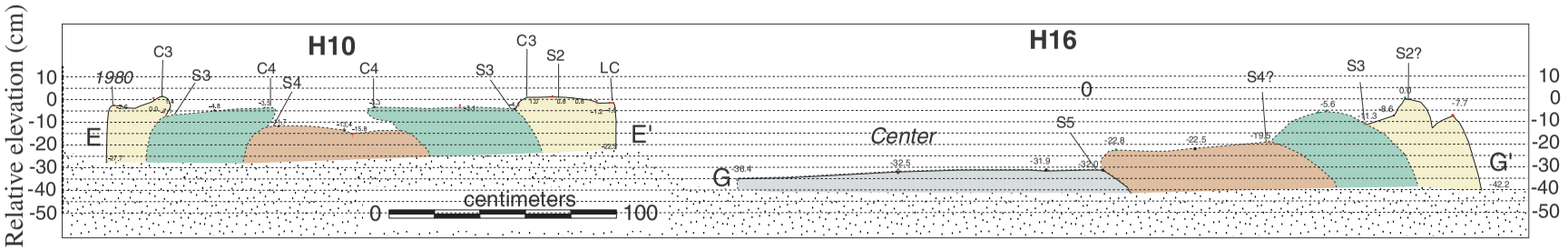

Figure 3.22b Cross sections of the large microatolls above. The interiors display a few lower flats indicative of general stable conditions interrupted by submergence event/episode.

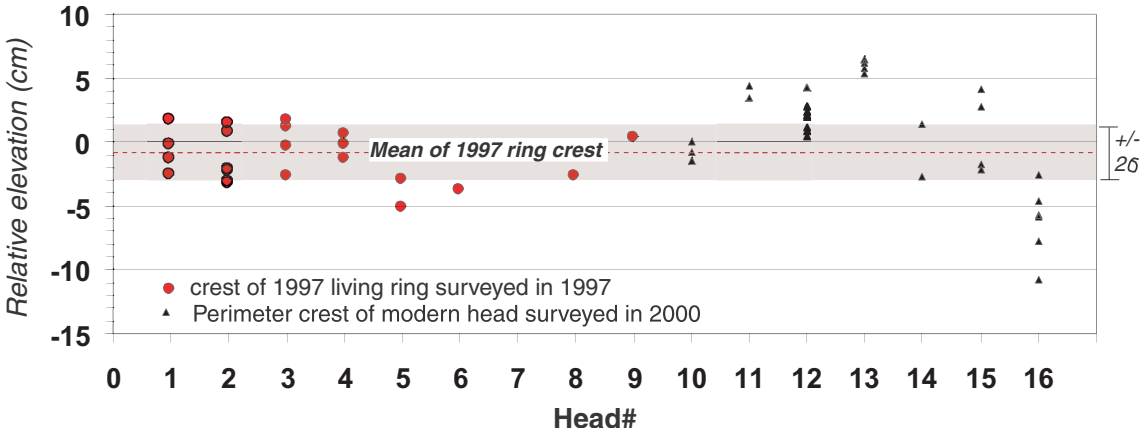

Figure 3.23a Tops of most of the microatolls are concordant. The elevations of the tops of living rings in 1997 are generally within 2 cm of each other.

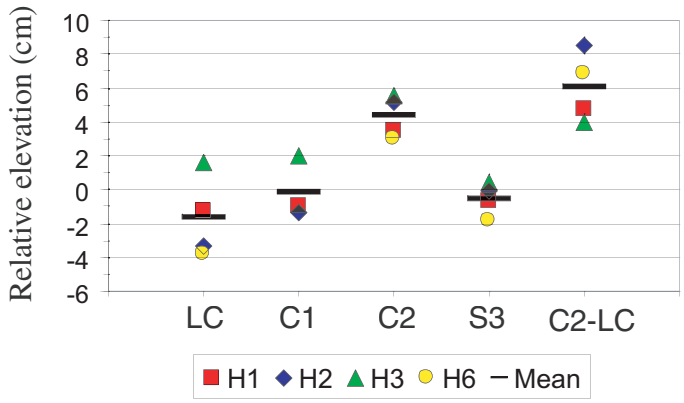

Figure 3.23b Comparisons of the elevations of similar crests and troughs across the heads shown in Figure 3.19b. It shows that most are concordant within 2 cm.

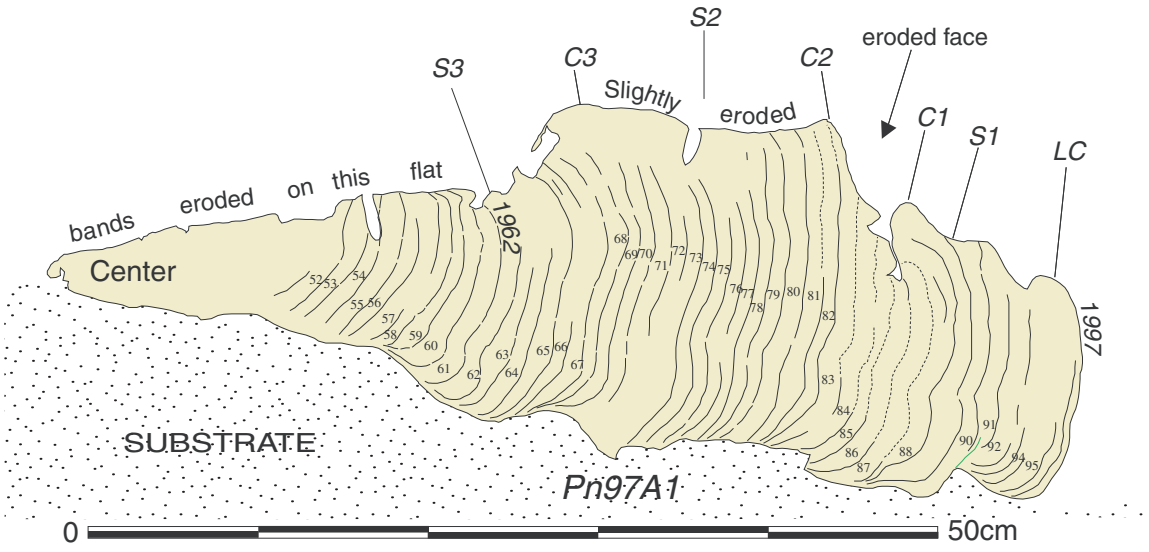

Figure 3.24 a Cross section of H2 showing rapid submergence in 1962, a stable period between 1969 and 1983, and rapid or sudden emergence about 1983-1986. Emergence persisted during the last decade. LC, S1, S2, S3, C1, C2, C3 are features indicated in Fig. 3.23b. The head was collected in July 1997.

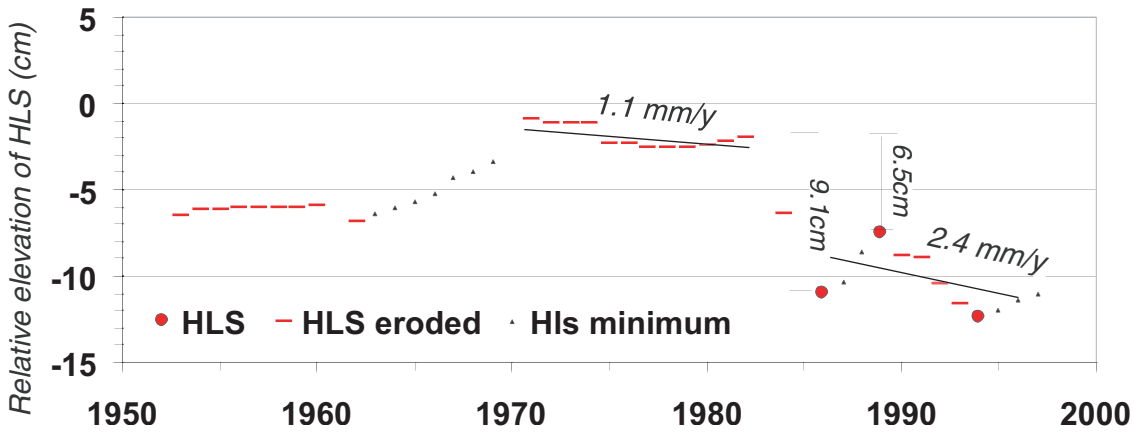

Figure 3.24b HLS history deduced from Pn97A1 slab.

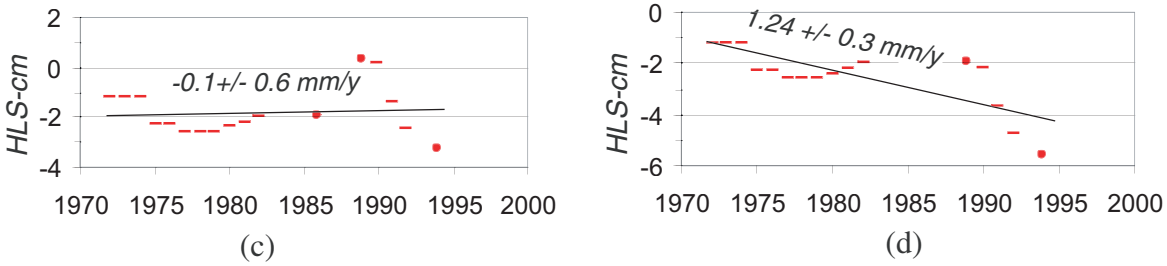

Figure 3.24 (c) and (d) Average rate if the effect of the mid-1980s emergence step is removed. (c) Assume the emergence is 9.1 cm. (d) Assume the emergence is 6.5 cm.

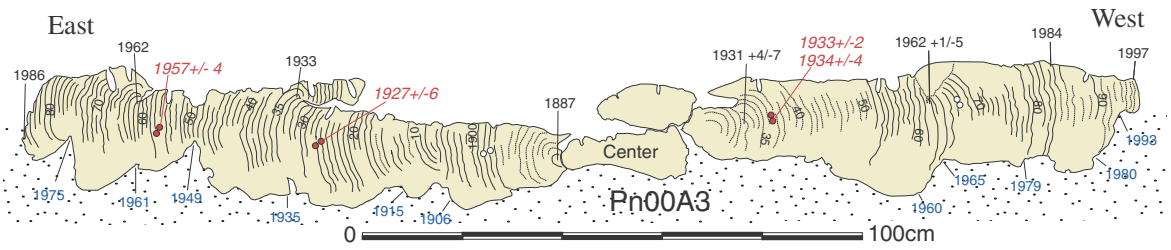

Figure 3.25a Cross section of the head H10 - Pn00A3.

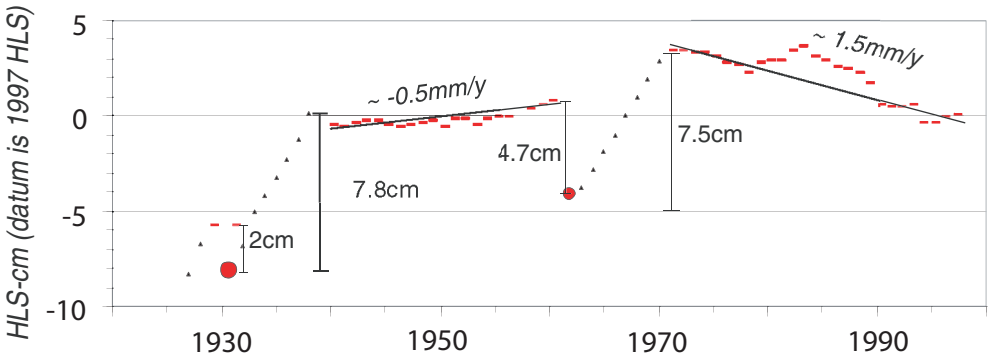

Figure 3.25b Plots of HLS records of the east wing as a function of time.

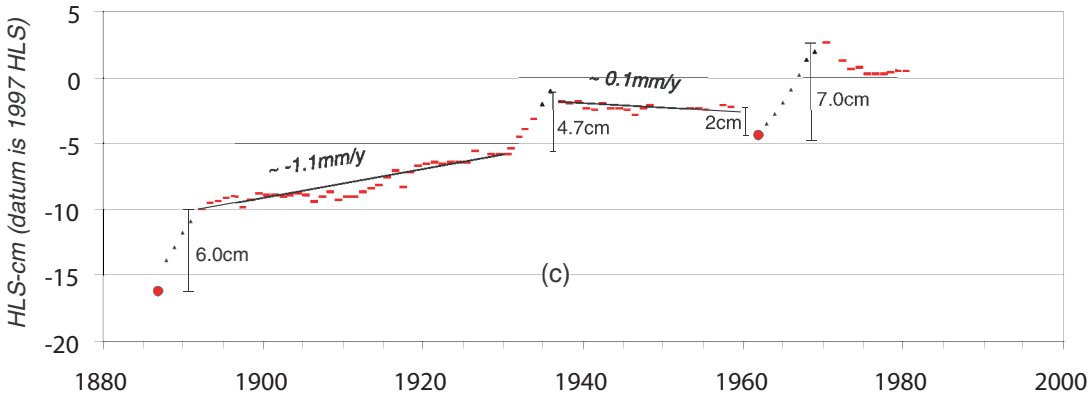

Figure 3.25c Plots of HLS records of the west wing.

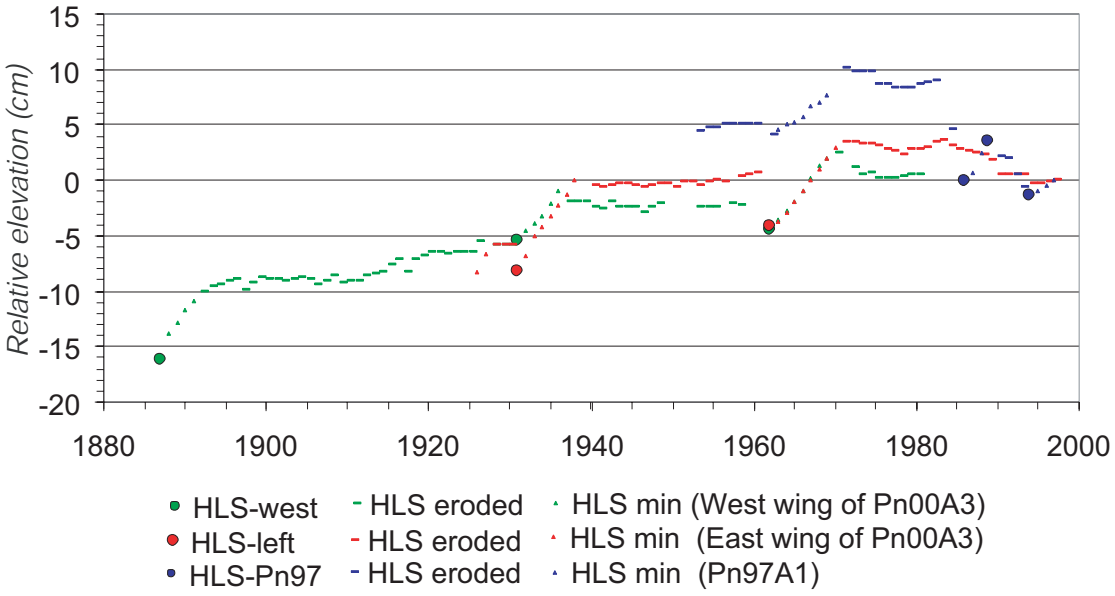

Figure 3.26a Combined HLS histories of Pn00A3 and Pn97A1. HLS histories of the west and east wings of Pn00A3 are generally similar. HLS history of Pn97A1 has a similar magnitude and timing, but at a distinctly higher level.

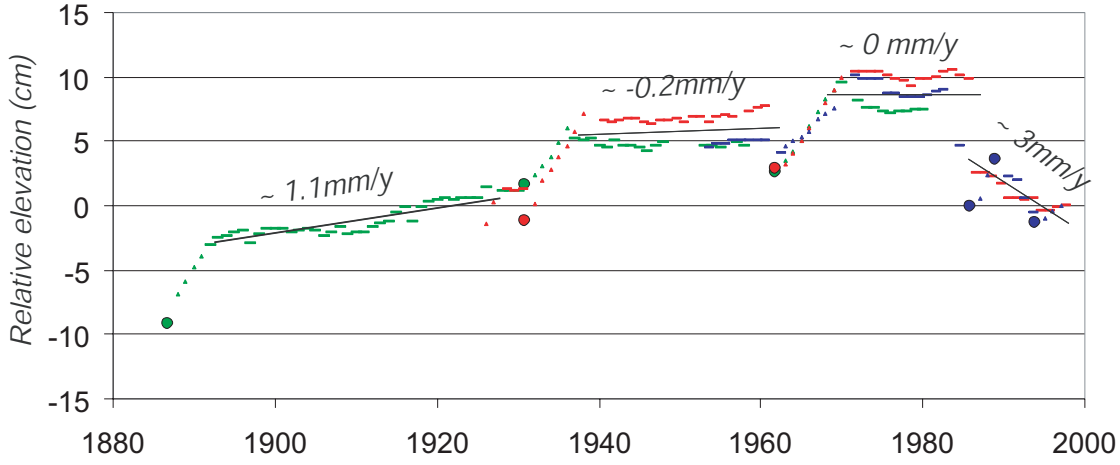

Figure 3.26b Combined HLS graph after correction for a possible 7 cm local settlement of the Pn00A3 head during the 1984 earthquake.

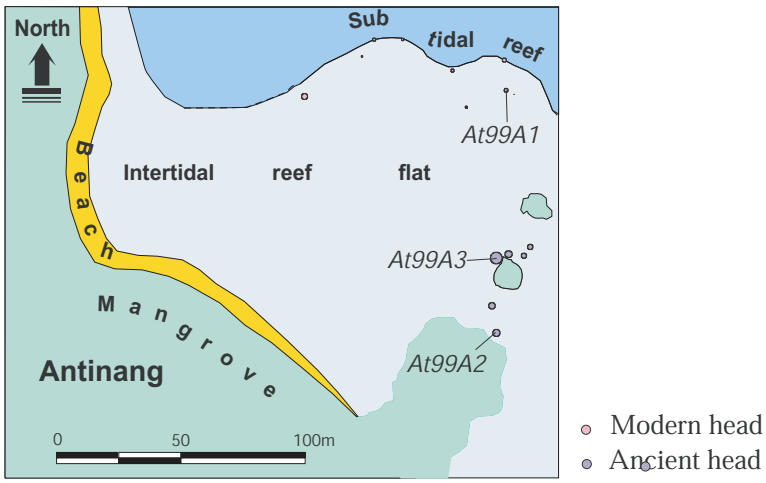

Figure 3.27 Antinang site. Modern heads are situated on the outer part of the intertidal reef. Mid-Holocene heads occupy the inner side of the shallow-muddy beach. These ancient heads grew to an elevation about 50 to 60cm higher than that of modern heads.

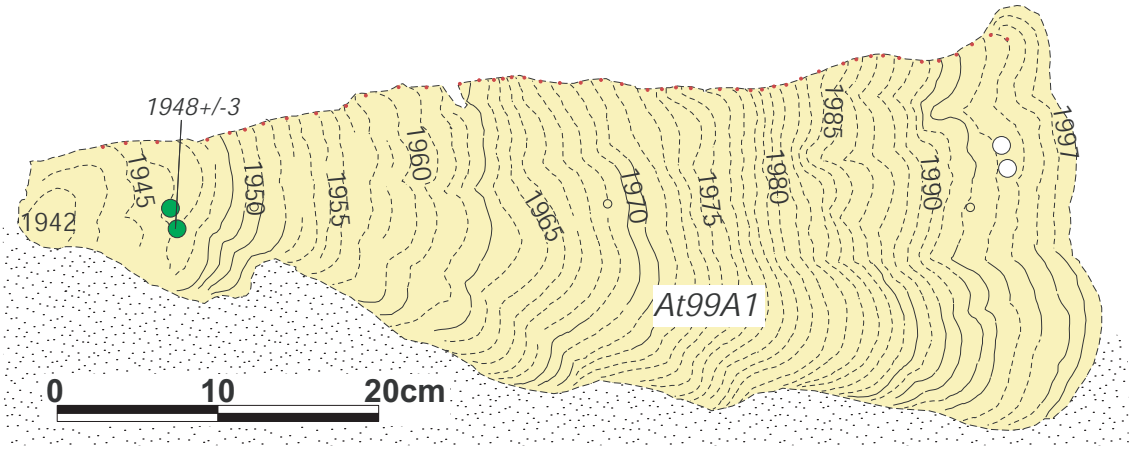

3.28(a)

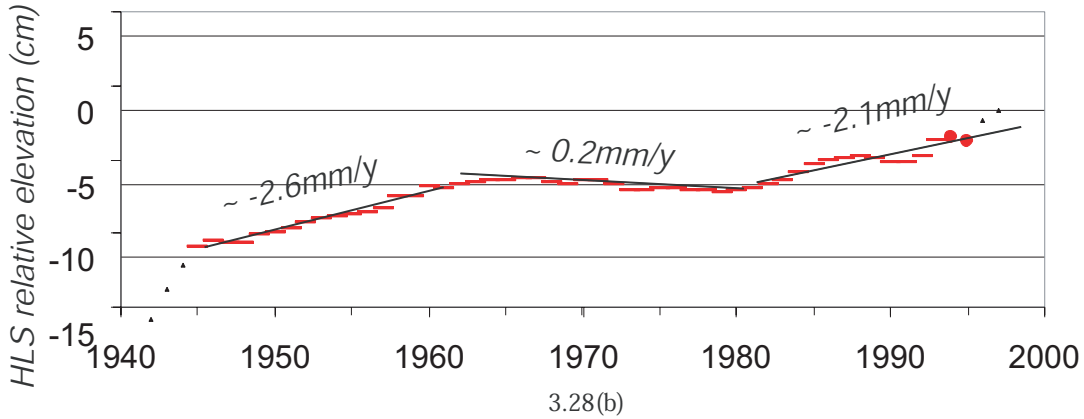

3.28(b)

Figure 3.28 (a) Trace of a radiograph of the At99A1 slab that was collected from a modern head. **(b)** Deduced HLS history showing slow submergence prior to 1960. Near-stable condition persisted from about 1960 to 1980. Submergence resumed from 1980 until recently.

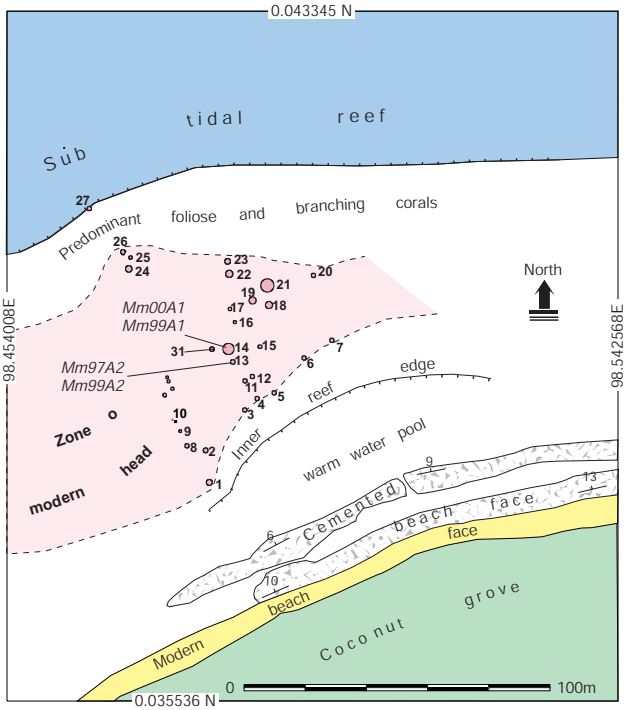

Figure 3.29 Map of the Memong site. Numbered pink circles represent heads surveyed in 1997, 1999, and 2000. *Porites* microatolls that were slabbed with a chain saw for more detailed analysis are labeled Mm99/00A1 and Mm97/99A2.

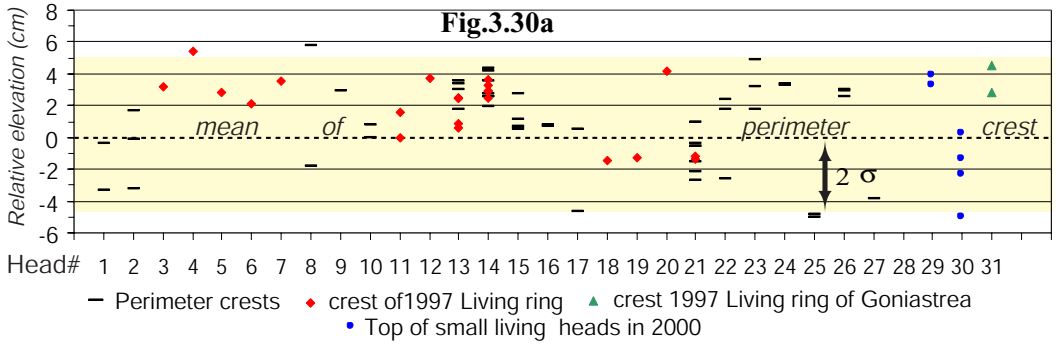

Perimeter crests (cm)	Fieldwork 1997			Fieldwork 2000		
	Mean	n	2 σ	Mean	n	2 σ
Head H13	4.6	5	± 2	2.9	4	± 1.6
Head H14	5.9	5	± 0.8	3.1	7	± 1.8
Intra head average	3.8	13	± 2.6	0.0	17	± 3.0
Inter head average	3.8	23	± 3.8	0.0	49	± 5.2

Fig.3.30b

Figure 3.30 (a) Graphical representation of relative elevations of 31 microatoll perimeter crests. Most are concordant within 5 cm of the mean value. **(b)** Table of relative mean elevations of perimeter crests and their uncertainty - in centimeters.

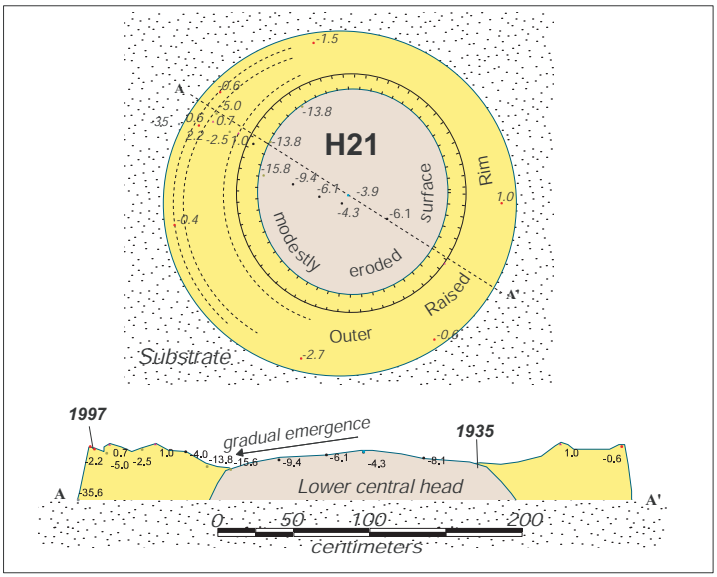

(a)

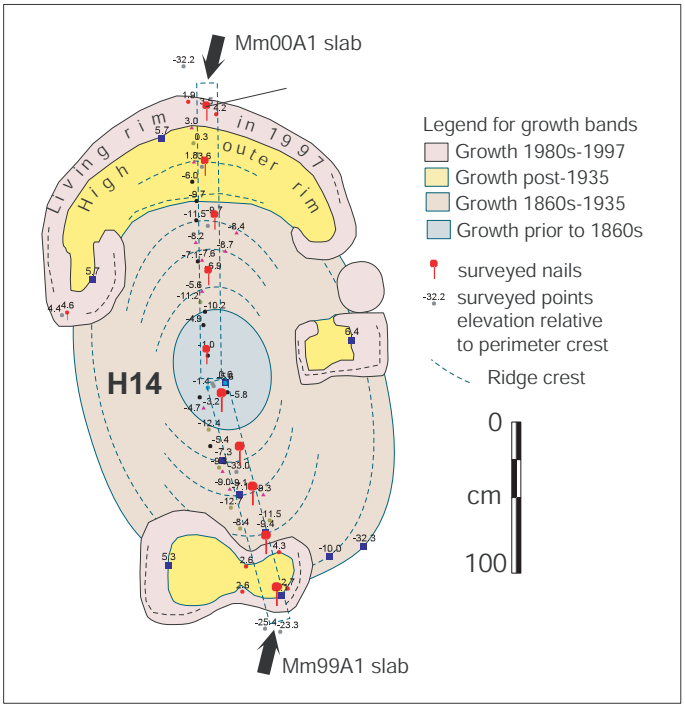

(b)

Figure 3.31 Maps of the two largest and oldest microatolls at the site. (a) Microatoll H21 was surveyed but not slabbed. Its contiguous and complete outer raised rim surrounds a gently outward sloping lower central head. (b) Microatoll H13 is elliptical and has a discontinued raised outer rim around a gently outward sloping inner disk. It also contains a central raised hemisphere. Two slab samples of the north and south radius of this head reveal details of the HLS history of the head.

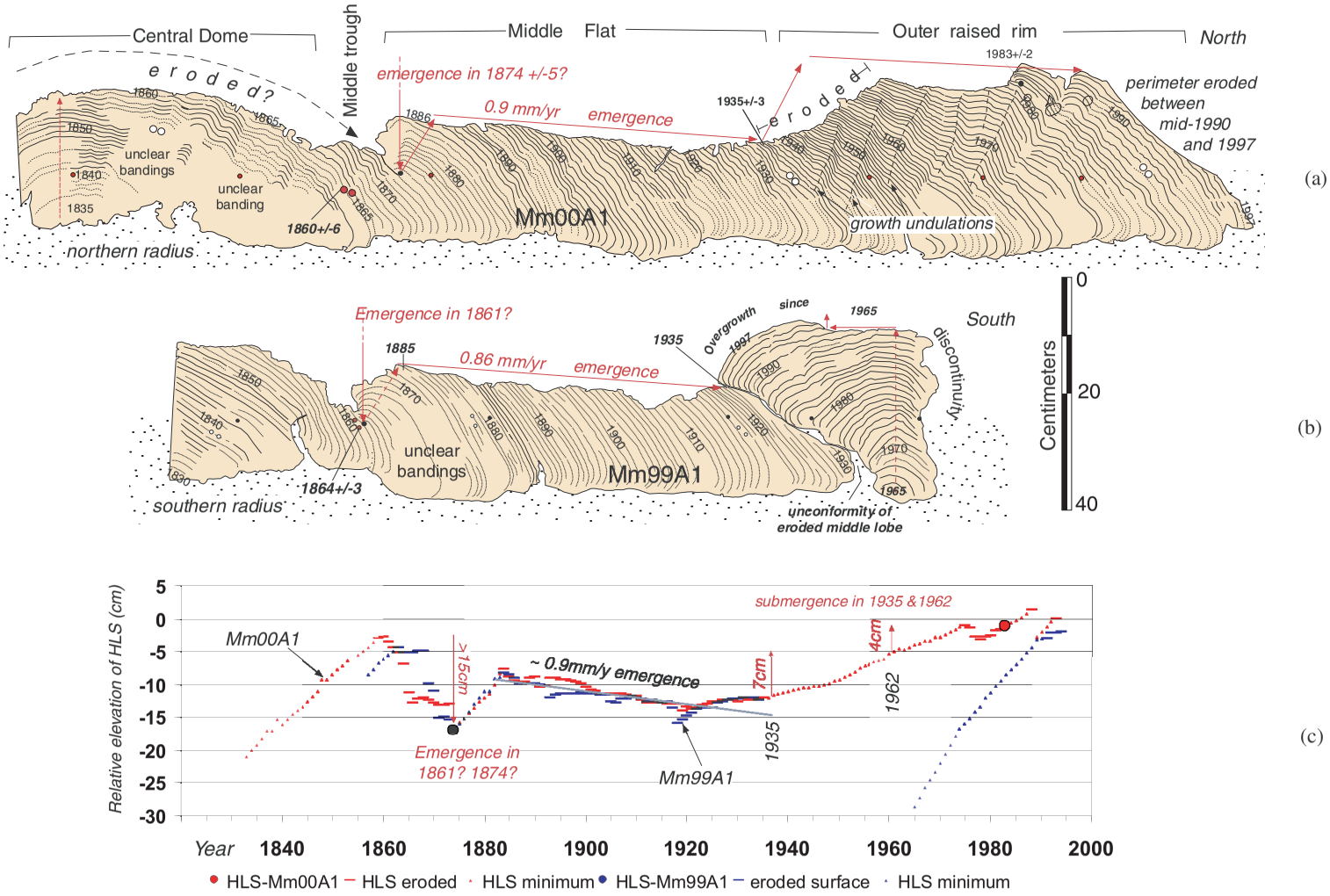

Figure 3.32 Tracings of the X rays from the two slabs. (a) The north radius has the most complete history. (b) The south radius reveals a similar history, but its usefulness is hampered by a break in the HLS record between about 1930 and 1990. (c) Together these two slabs reveal a lengthy period of slow, steady emergence (1885-1935), an episode of emergence followed by submergence (1860s and 1870s), and an episode of submergence (1935-1975).

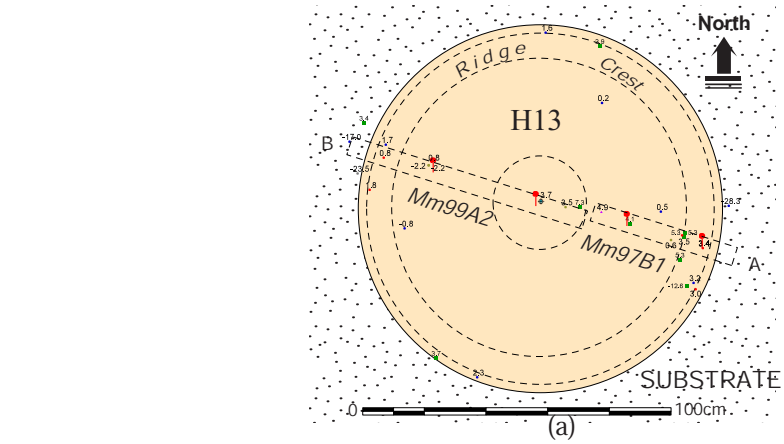

(a)

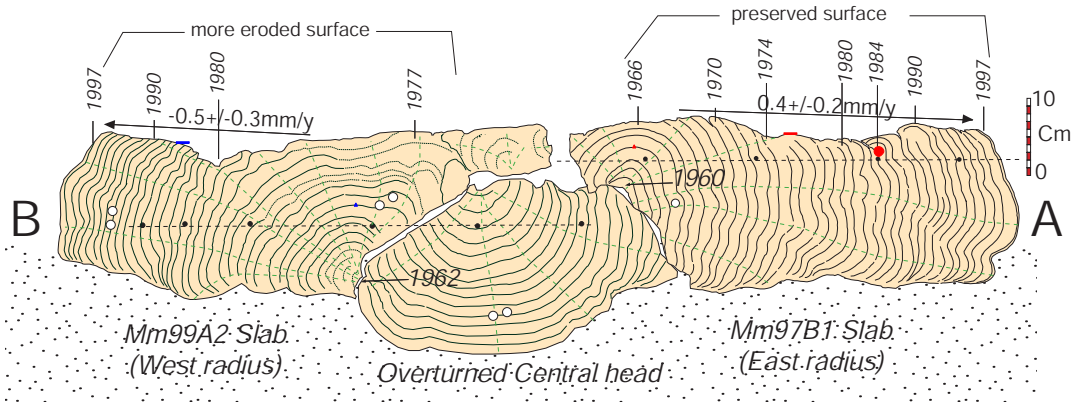

(b)

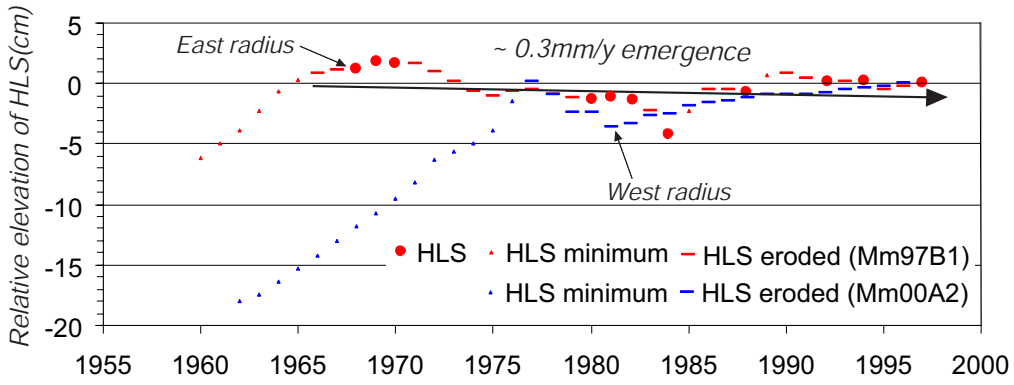

(c)

Figure 3.33 (a) Map view shows the nearly circular shape of the head H13. **(b)** Interpretation of radiographs of the sawed slab. The head was overturned sometime before 1960. Re-colonization of the head began in 1960 on the east radius and in 1962 on the west radius. Growth on the east and west radii reached HLS in 1966 and 1977, respectively. The record of HLS is longer and more accurate on the east radius. The average rate of emergence since 1966 has been about 0.4 mm/yr. **(c)** Two HLS histories from the east and the west wings are similar. Lower elevations of the west wing (Mm99A2) indicate some erosion. The site has been near stable for the last 3 decades (0.3 mm/yr emergence).

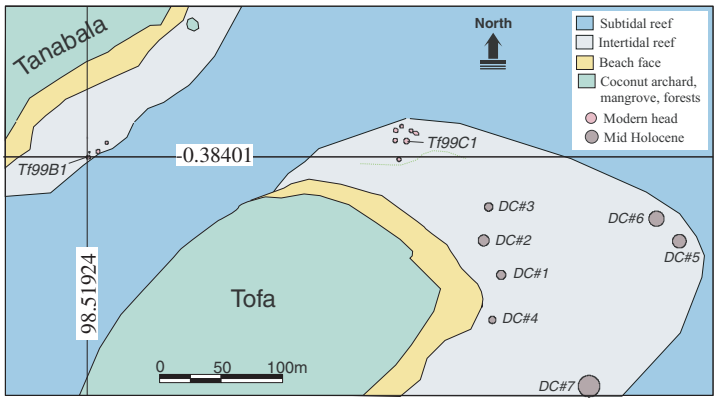

Figure 3.34 Site map at Tofa displays populations of both modern and mid-Holocene heads. These ancient heads grew to elevation more than 20 cm above that of modern ones.

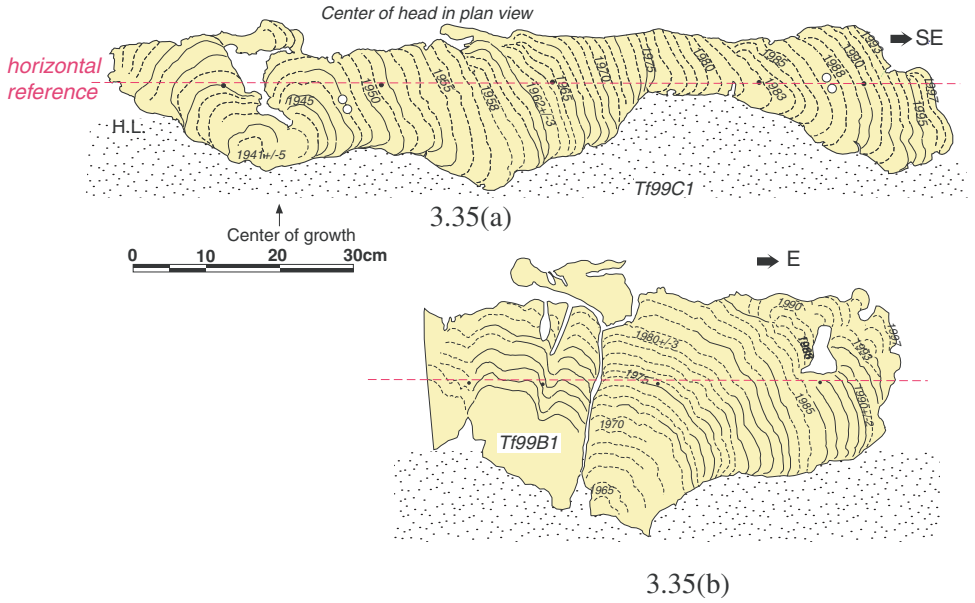

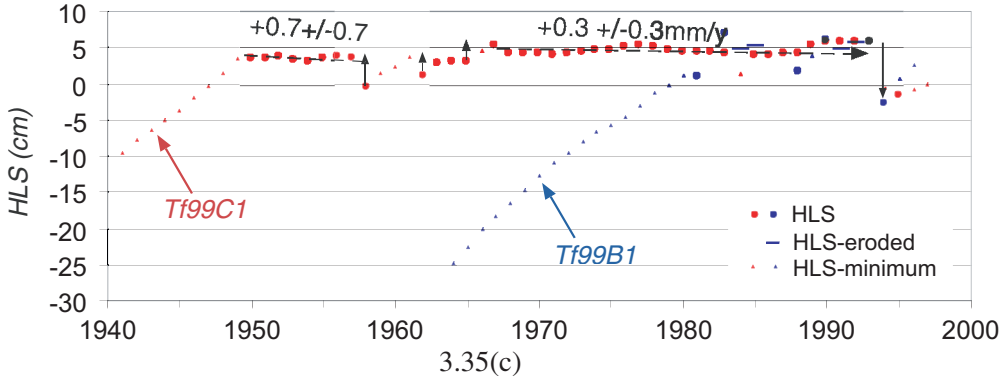

Figure 3.35 (a) Tf99C1 slab shows a non-symmetric growth pattern. The low relief of the head's topography implies general near-stable condition for the past 50 years. Periods of rapid submergence occurred in early 1940s, late 1950s, and in early 1960. (b) Tf99B1 slab shows a similar HLS history for the past 15 years. (c) HLS history derived from the two modern heads.

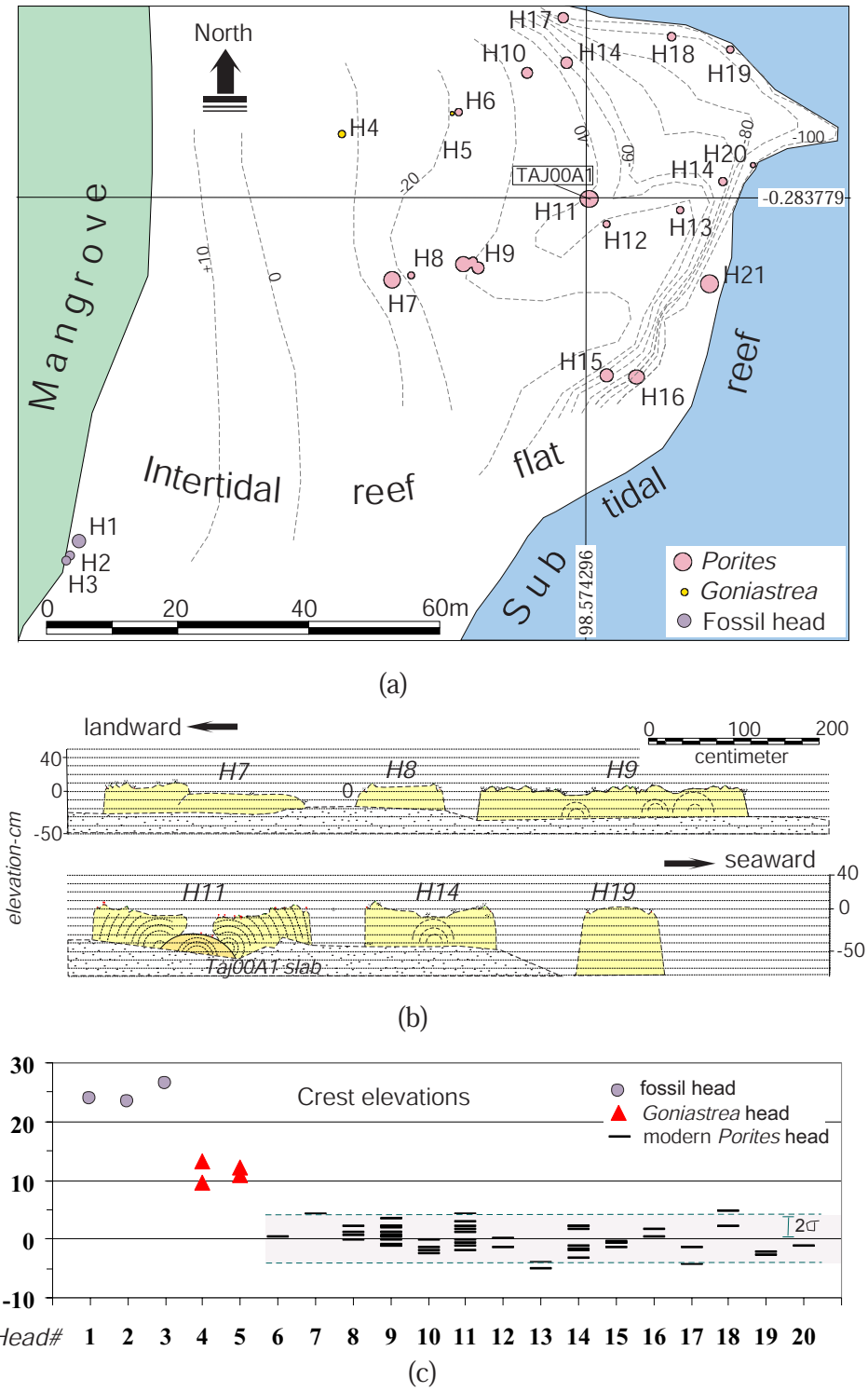

(a)

(b)

(c)

Figure 3.36 (a) Site map in Tanjung Anjing near the southeast corner of Tanamasa Island **(b)** Head cross sections showing a general morphology of Porites microatolls. Outer rise step at H11 indicates a major submergence in 1935. **(c)** Surveyed elevations of head's crests. Crests of modern heads are aligned within ± 2 cm (2-sigma uncertainty). Goniastrea's crests are 10cm higher than those of Porites. Crest of old heads near the mangrove line are higher still.

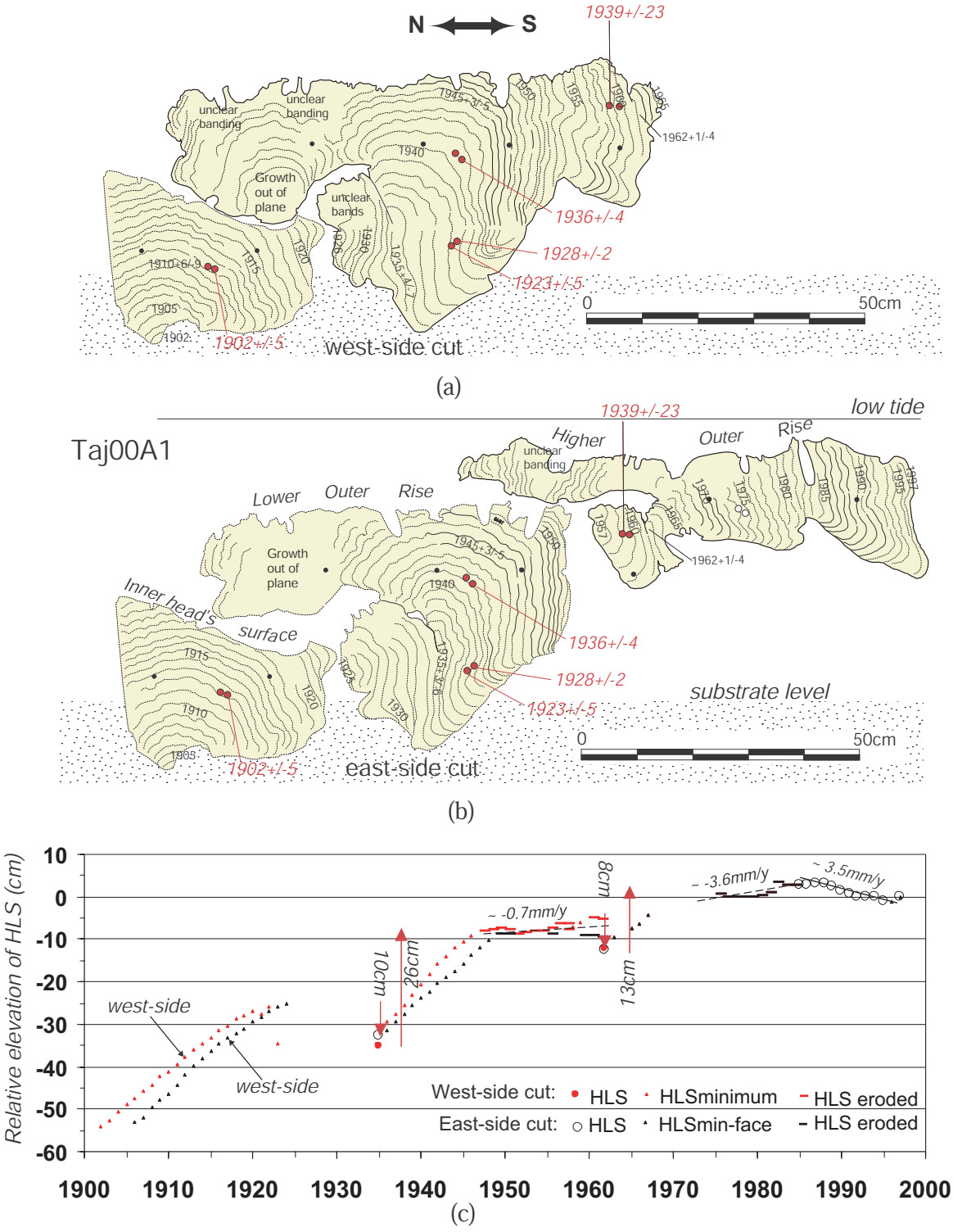

Figure 3.37 (a) Trace of the radiographs of a thin cut of the west side of the thick slab collected from a modern head at Tanjung Anjing. Age assignments assume 1997 for an exterior ring. Red numbers are dates from U-Th geochronometry. **(b)** A thin cut of the east side of the slab. Overall geometry shows a non-uniform submergence. It includes three levels of flat surfaces: the pre-1935 central-low, the intermediate pre-1962 bands, and the post-1962 outer-rise rim. (c) HlS histories of the two cuts.

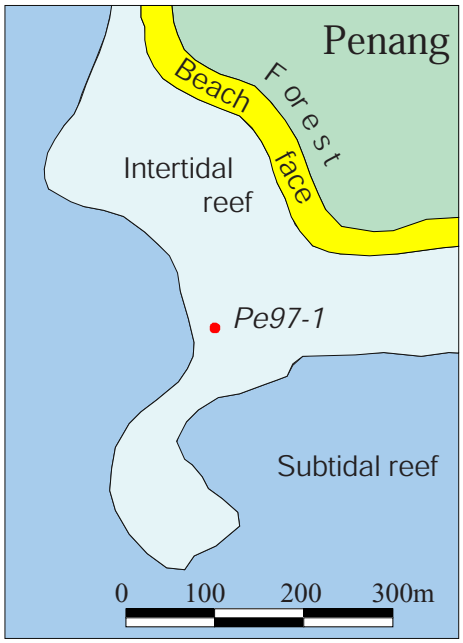

Figure 3.38 Site map of Penang Island.

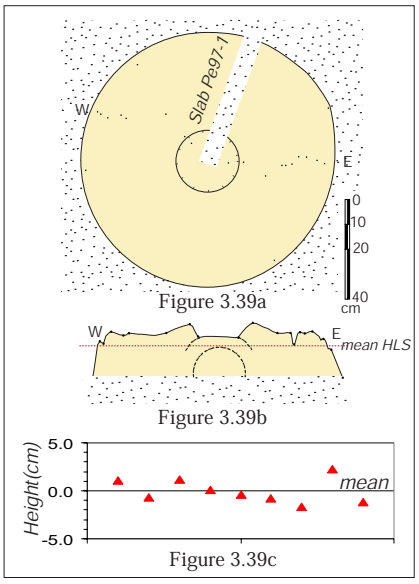

Figure 3.39 (a) and (b) Slabbed modern head and its cross-section. **(c)** Relative elevation of the crests of living rings surveyed in mid-1997.

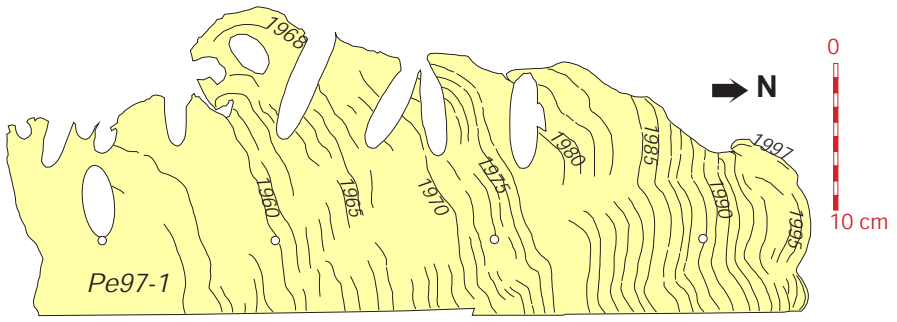

3.40(a)

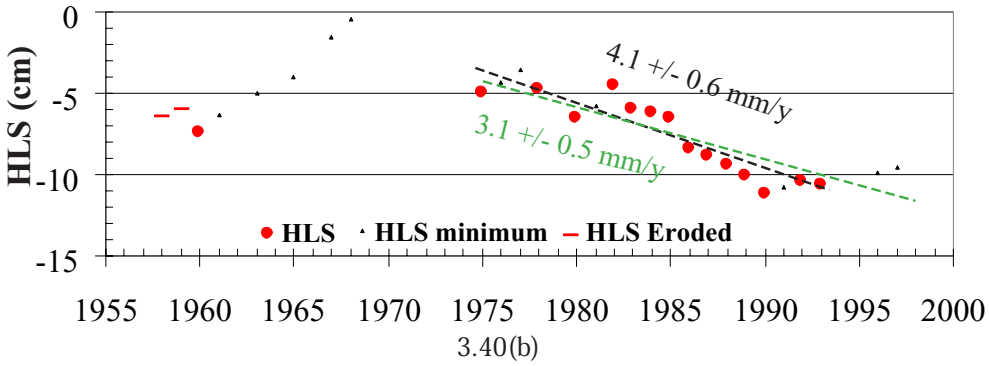

3.40(b)

Figure 3.40 (a) Pe-97-1 slab shows emergence and larger submergence events in 1960. Emergence has persisted for the last 30 years. **(b)** Least-squares averaged emergence is about 3 mm/yr if using only HLS records and about 4 mm/yr if including minimum HLS in 1996 and 1997.

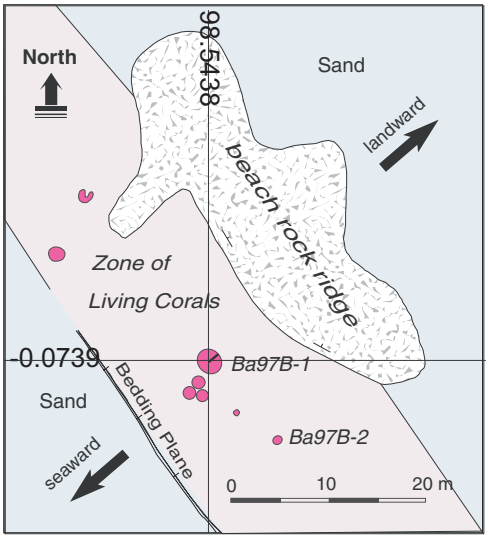

Figure 3.41 This site, on a small islet in northern tip of Bai Island exposed only during lowest tides, shows the relationship of selected living coral heads to the rocky and sandy substrate and to each other. The location of slab Ba97B1, cut from one coral head is shown as a black line.

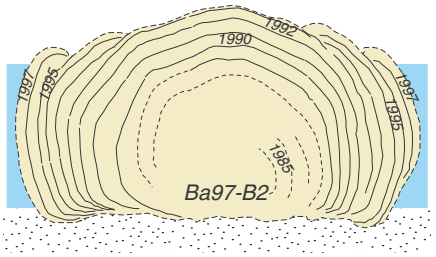

Figure 3.42a The "cabbage" head.

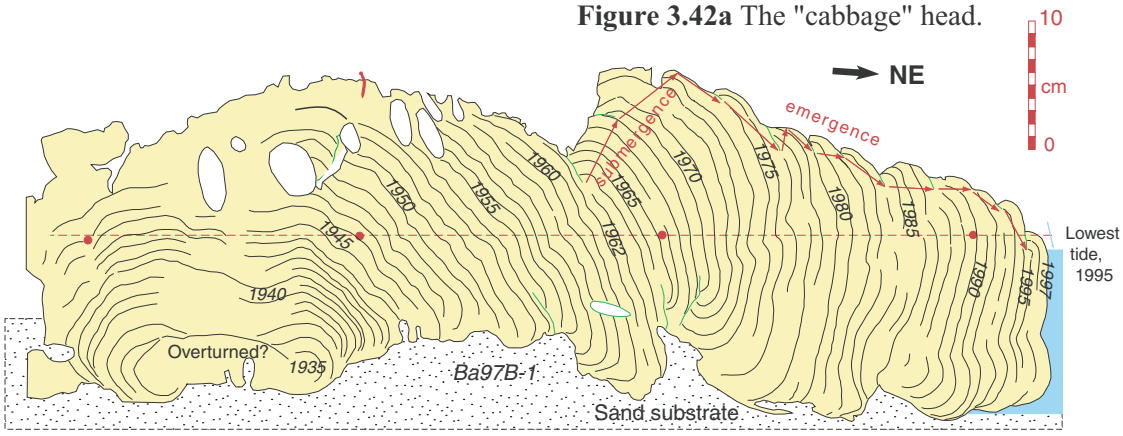

Figure 3.42b

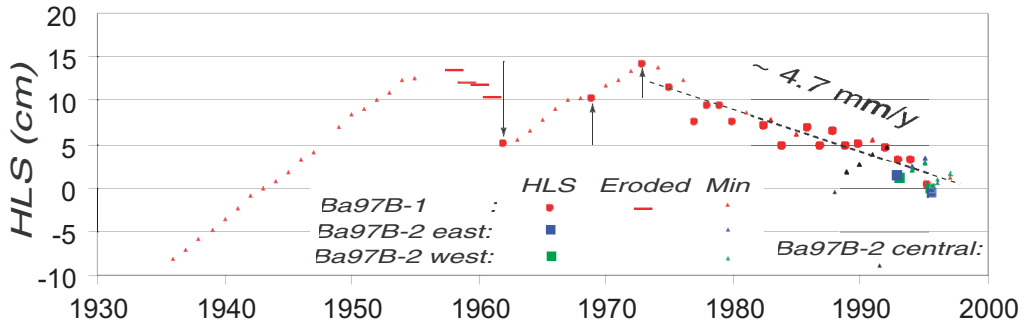

Figure 3.42c

Figure 3.42b The cross section of this larger slab reveals a clear record of annual growth bands. The slab shows radially outward growth at about 1 cm/yr. The rise and fall of HLS of the coral during the past 40 years is reflected in the topography of the upper surface of the coral head. The red arrows track the rise of sea level in the 1960s and its subsequent fall. (c) Rapid emergence at about 4.7 mm/yr has been occurring since about 1973. In about 1960 either a sudden submergence occurred or a decade-long episode of rapid submergence began.

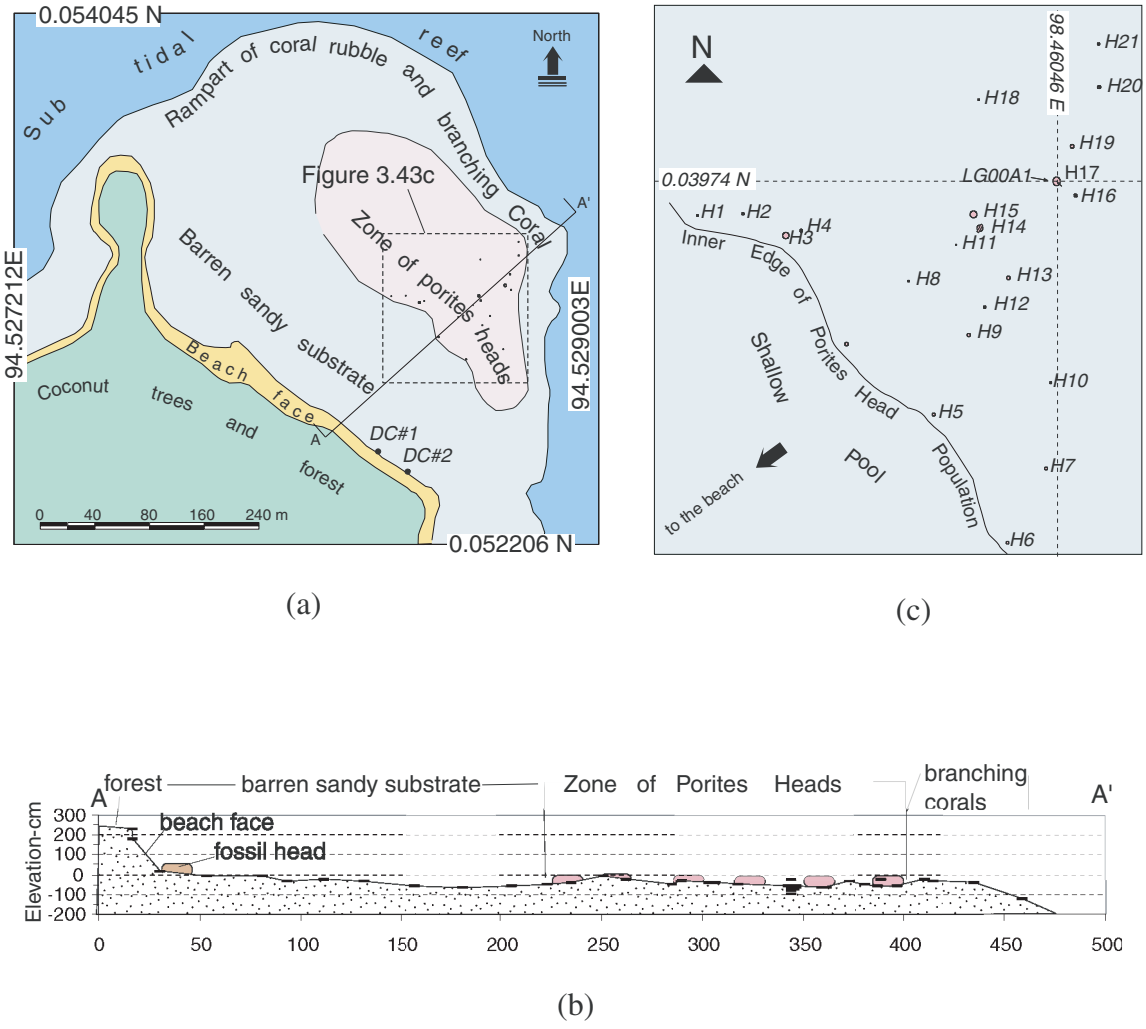

Figure 3.43 Map and profile of the Lago site, on the northeastern flank of Lago Island. (a) A field of Porites heads occurs on the broad intertidal reef flat, behind a high-energy rubbly rampart. DC#1 and DC#2 are the locations of the old heads where we took drill core samples. (b) Schematic beach cross-section. (c) Detailed map of the field of the modern Porites heads that we surveyed in 1999 and 2000.

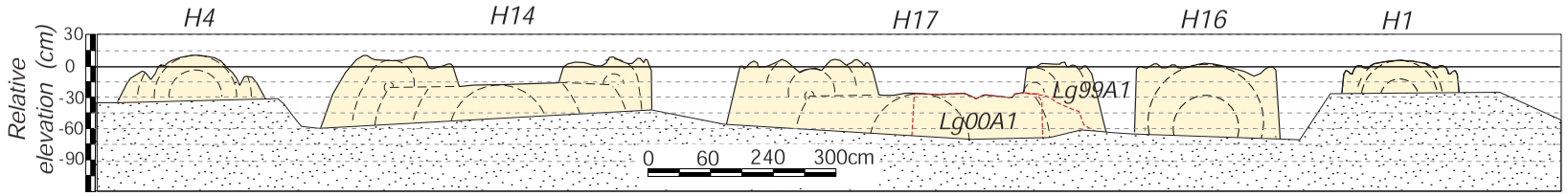

3.44(a)

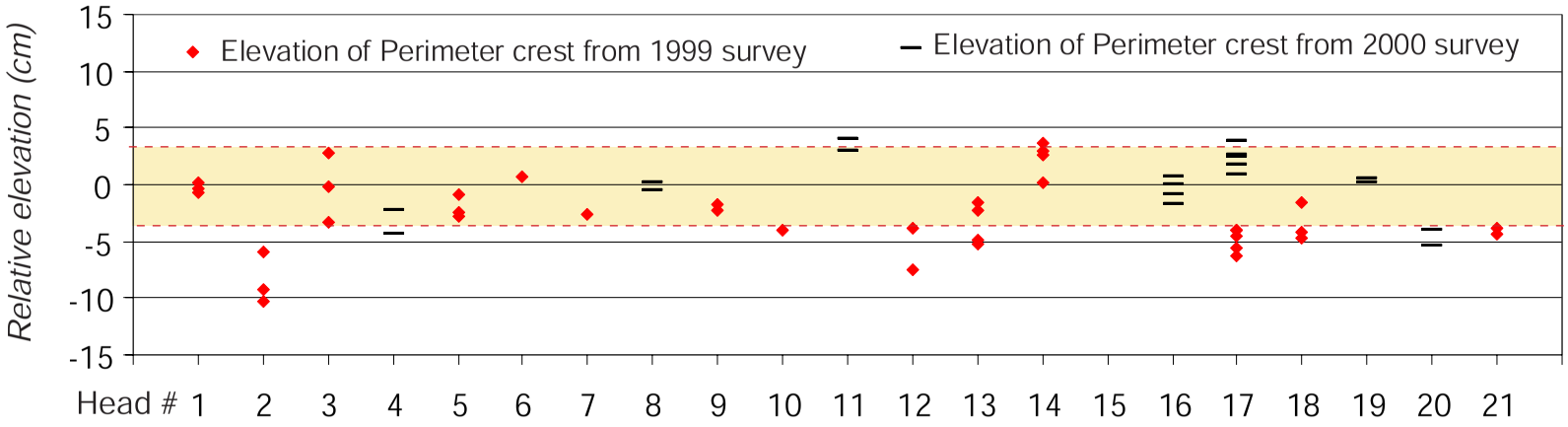

3.44(b)

Figure 3.44 Profiles of four selected microatolls and measurements of perimeter crest elevations of 21 heads. (a) Smaller heads formed after the large submergence event of 1935. Thus, they lack a low inner flat. Their shape indicates slow emergence in the past few decades. The cup-shaped morphology of the larger heads results from about 30 cm of submergence in 1935. The low inner flat pre-dates 1935, whereas the raised outer rim post-dates 1935. (b) Relative elevations of the perimeter crests of 21 microatolls surveyed in 1999 and 2000. The crests deviate from their mean by only ±3cm (2 s).

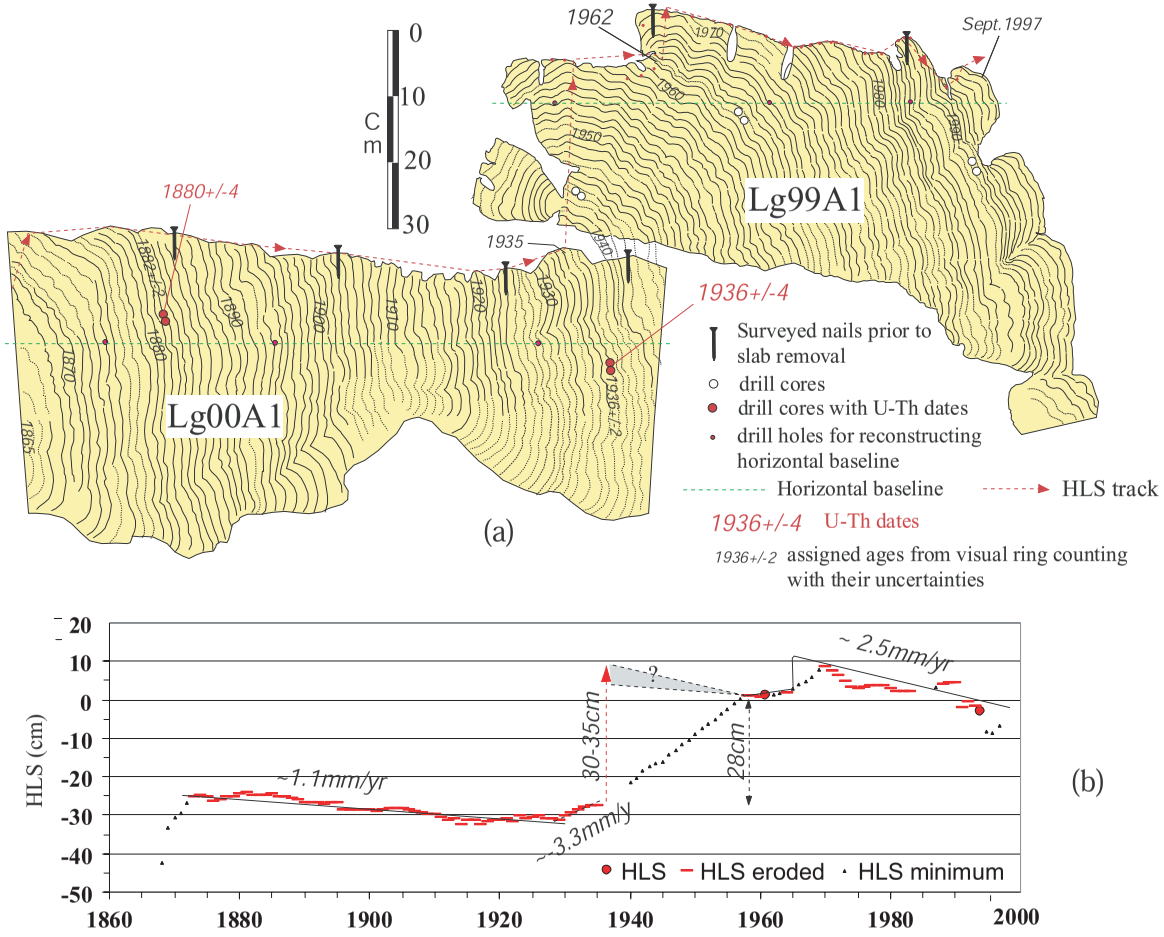

Figure 3.45 Slabs from head H17 (a) Two slabs, Lg99A1 and Lg00A1, collected in 1999 and 2000. The top of central lower flat suggests slow emergence site between 1873 and 1920. Sudden or rapid submergence in 1935 resulted in free upward growth of about 30 cm from 1935 to 1957. The flats of the outer rim represent growth from about 1958 to 1961 and from 1970 to 1997. The 8 cm rise in the height outer rim between 1962 and 1970 resulted from submergence in 1962. Dates of bands are assigned based on visual ring counting assuming the exterior band formed in 1997. (b) Plot of the HLS history recovered from Lg99A1 and Lg00A1. Note the sizes of the submergence events in 1935 and 1962 and notice that the post-1970 emergence rate is twice as fast the pre-1935 rate.

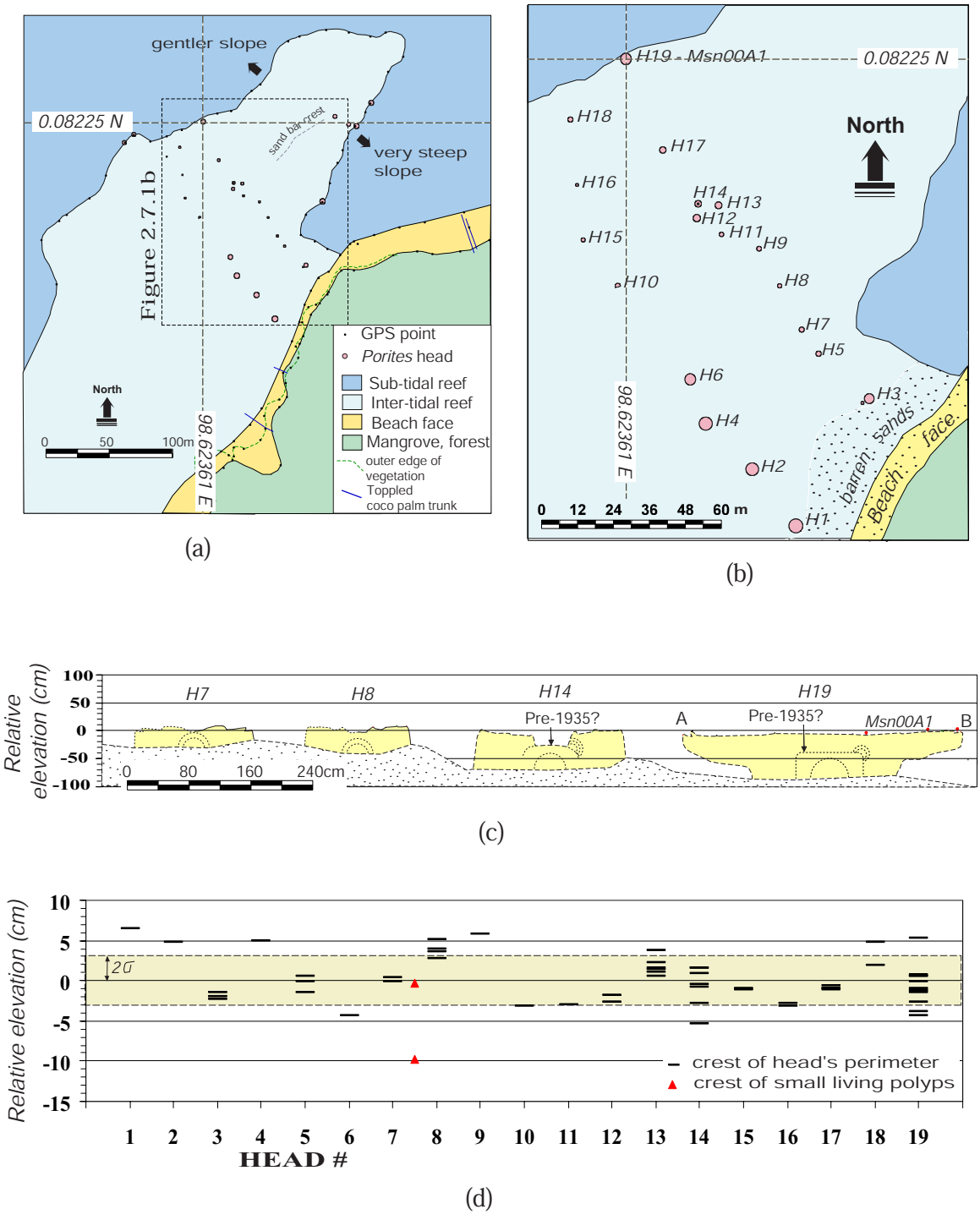

Figure 3.46 (a) General map of Masin site. **(b)** Detailed map of surveyed modern microatolls. **(c)** Cross- sections of the selected heads. A rapid submergence in 1935 is indicated by topography of head H14. Flatness of surface tops implies many decades of a stable condition. **(d)** Elevation of the perimeter's crests are concordant within ± 3 cm (2-σ uncertainty).

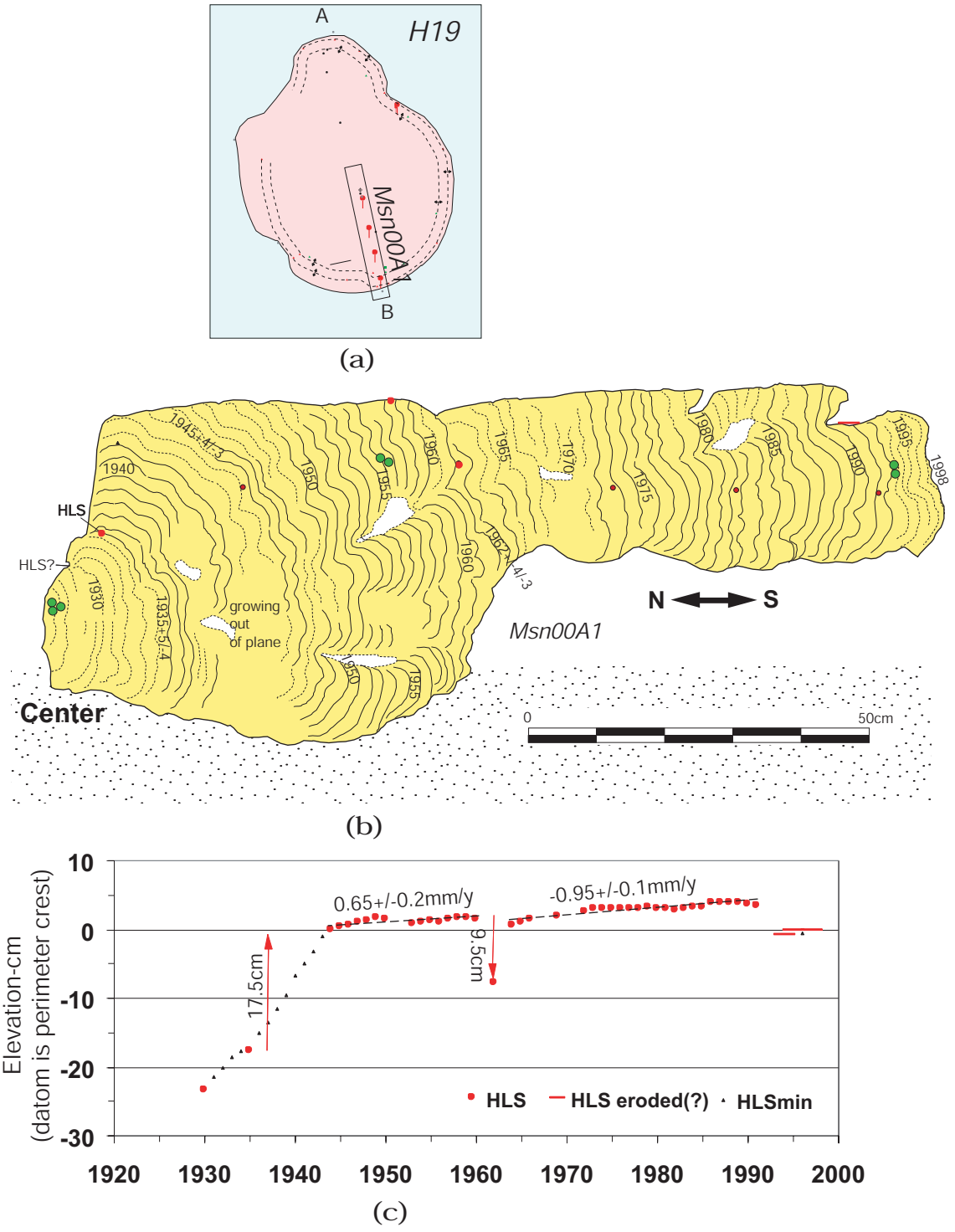

Figure 3.47 (a) Plan-view map of head H 19 and the location of collected slab. (b) Trace of the radiography of the Msn00A1 slab. HLS impingement occurred in 1930, 1935, and from 1943 to recent time. MAjor events are recorded in 1935 and in 1962. (c) HLS history depicted from the slab.

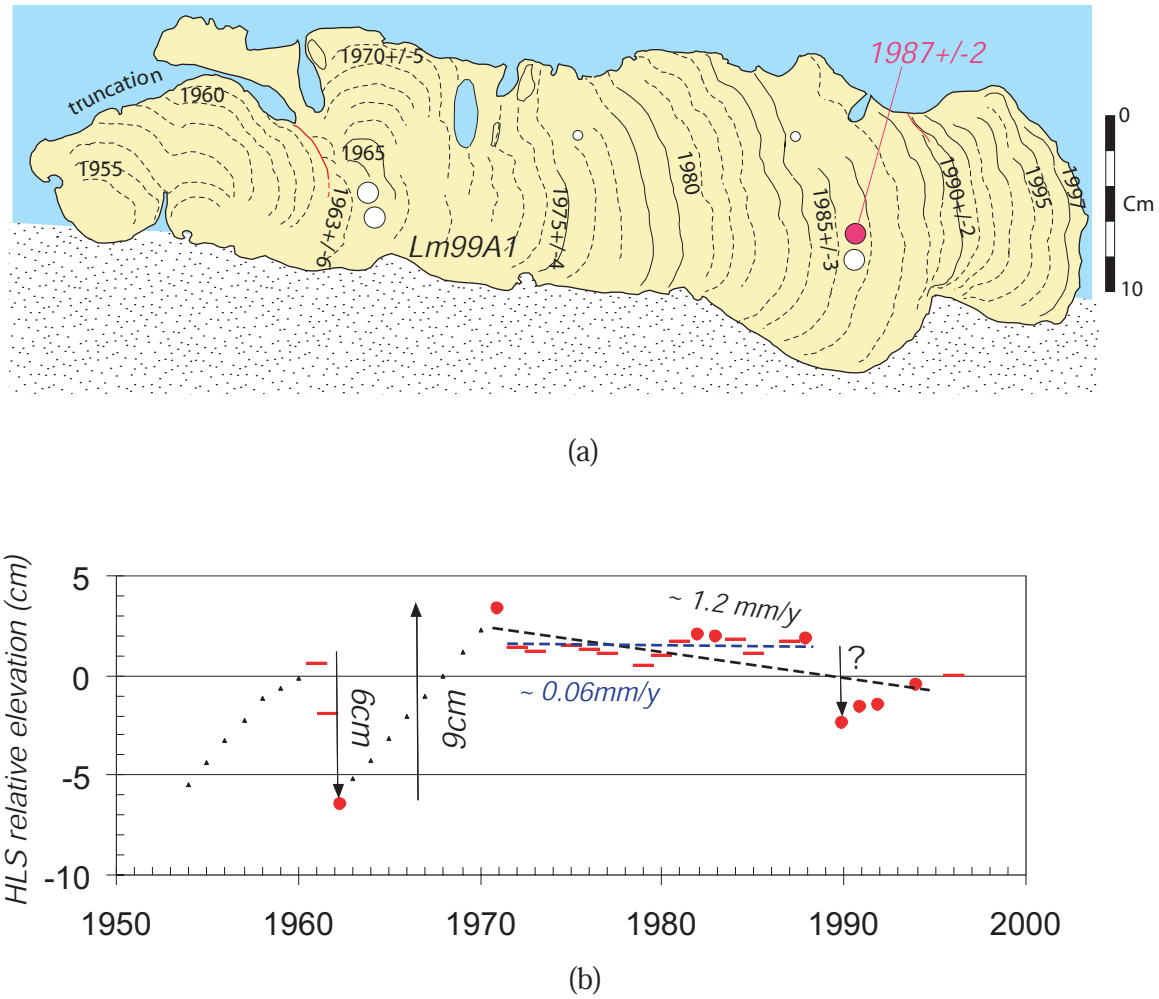

Figure 3.48 (a) Coral stratigraphy from the modern head indicates emergence and larger submergence event in 1962. (b) A least-squares fit to HLS impingement from 1971 to 1997 yields an average emergence rate of about 1.2 mm/y. If one exclude the local emergence in 1990, the average emergence rate is near zero (~0.06 mm/yr).

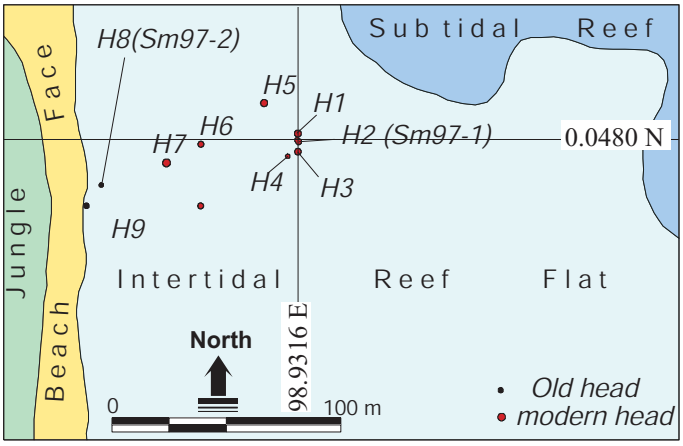

(a)

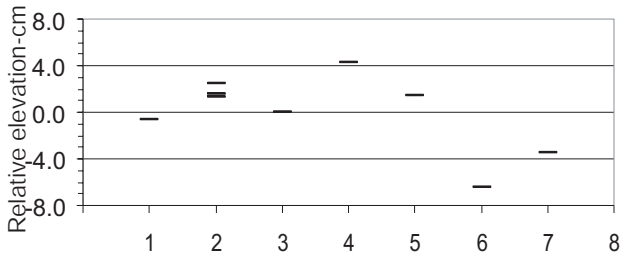

(b)

Figure 3.49 (a) Map of site at Sambulaling. Modern heads occupy most of region between the outer rampart and the beach. A smaller population of older head settles near the beach berm. (b) Survey of crests of living rings in 1997 showing that they are concordant within 2 cm.

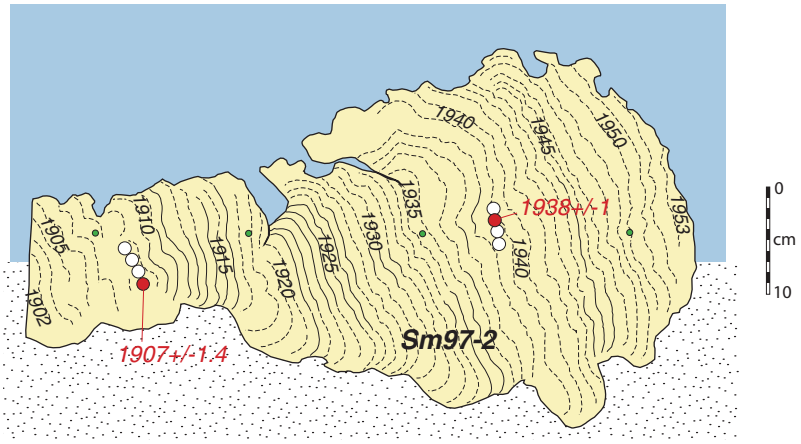

Figure 3.50a An internal growth structure of Sm97-2 slab collected from old head H8. It reveals a period of near stability prior to 1935 and a rapid submergence between 1935 and 1950. Significant HLS impingement occured in about 1920, 1935, and 1945. Microatoll died in the early1950s.

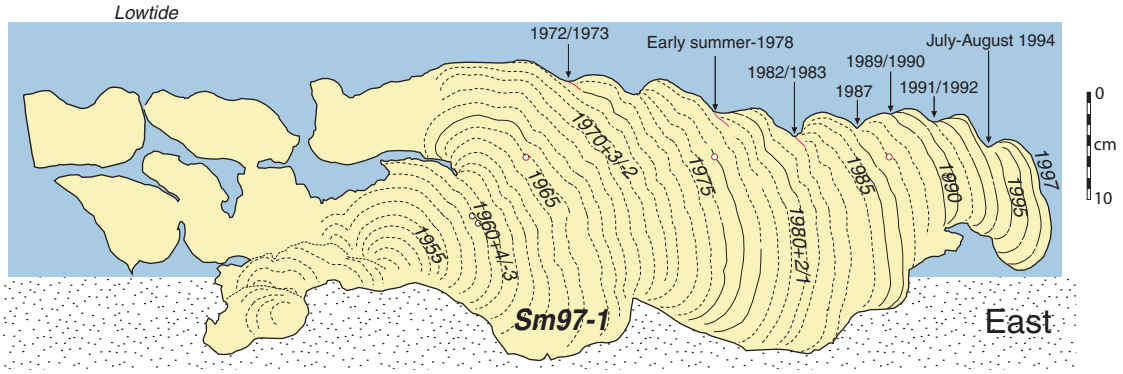

Figure 3.50b Cross section of the modern head H2. Emergence occured in about 1961, and it was followed by unhindered upward growth that is attributed to a larger submergence event. Topography of coral bands between 1971 and 1997 showing preserved smal ridges and throughs that represent minor fluctuations of HLS.

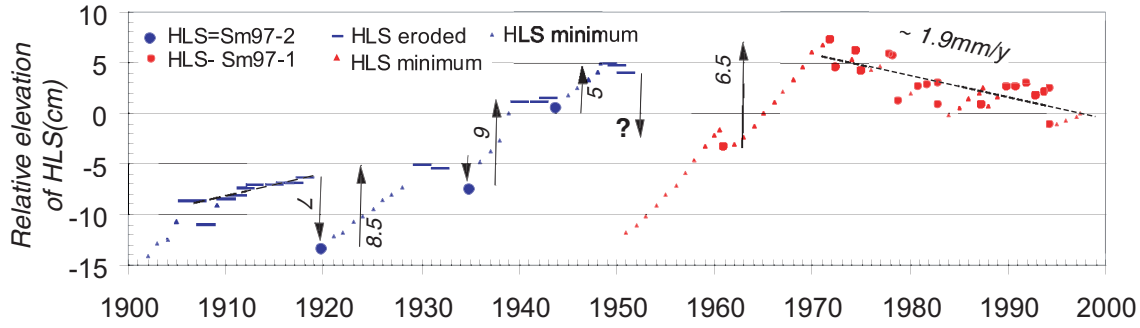

Figure 3.50c Graphical representation of combine HLS history derived from the old and modern microatolls, spanning almost the entire 20th century. A least-squares fit to HLS between 1971 and 1997 yields an average emergence rate of about 1.9 mm/yr for the past three decades.

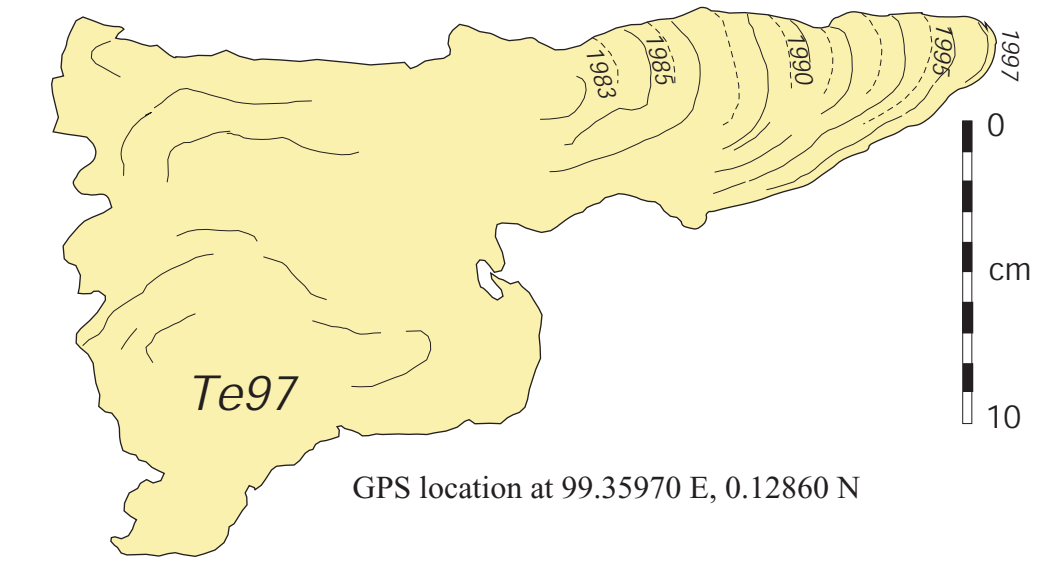

(a)

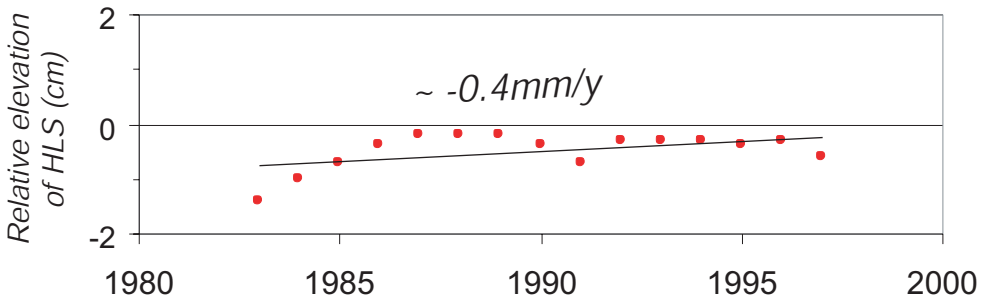

(b)

Figure 3.51 (a) Chisseled sample from a small living head in mid-1997 at the Telur site. A near flat topography of the upper surface indicates recent stability. Banding is unclear, except along the the outermost 15 cm. (b) HLS history for the past 15 years.